Chemical vapour deposition and thin film growth

Ausrine Bartasyte

FEMTO-ST Institute, University of Franche-Comté,
Besançon, France
ausrine.bartasyte@femto-st.fr

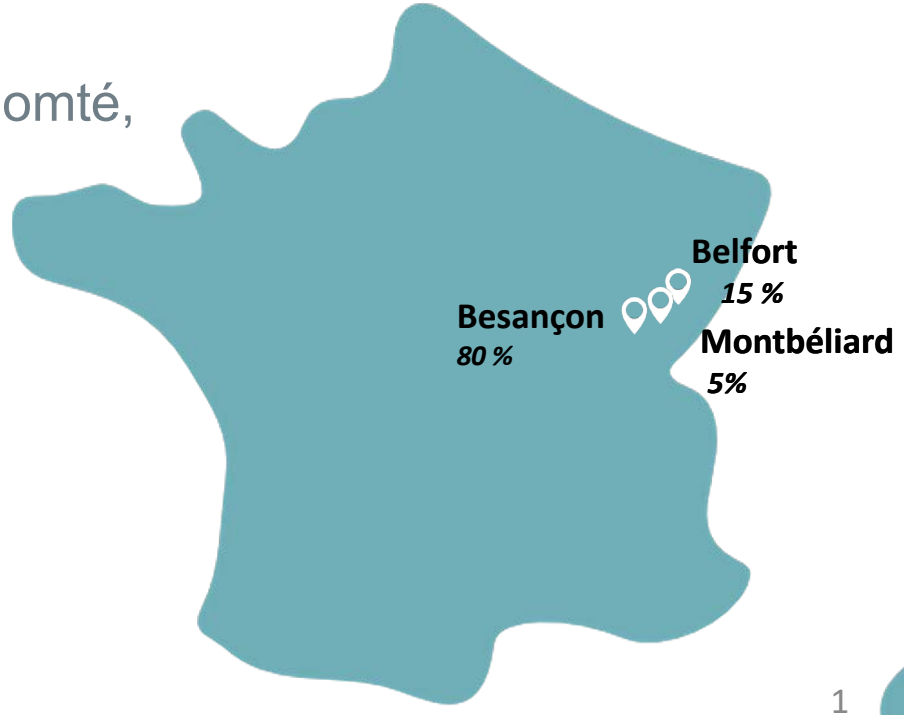

Outline

- Chemical vapour deposition
  - Definition
  - Precursors & delivery systems
  - Thin film growth mechanisms
- Structure and properties of thin films
  - Structure and orientation
  - Defects & composition
  - Residual stresses

Chemical vapor deposition

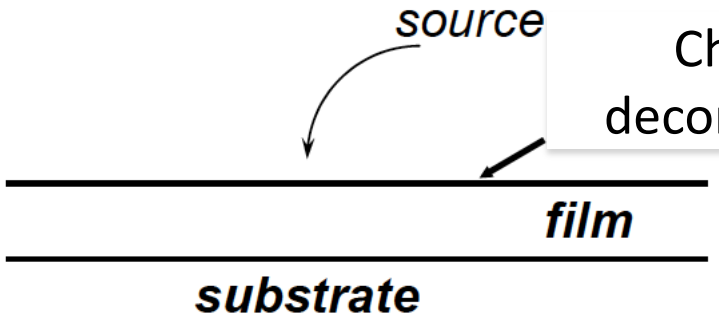

Chemical reaction between (or decomposition of) volatile molecules

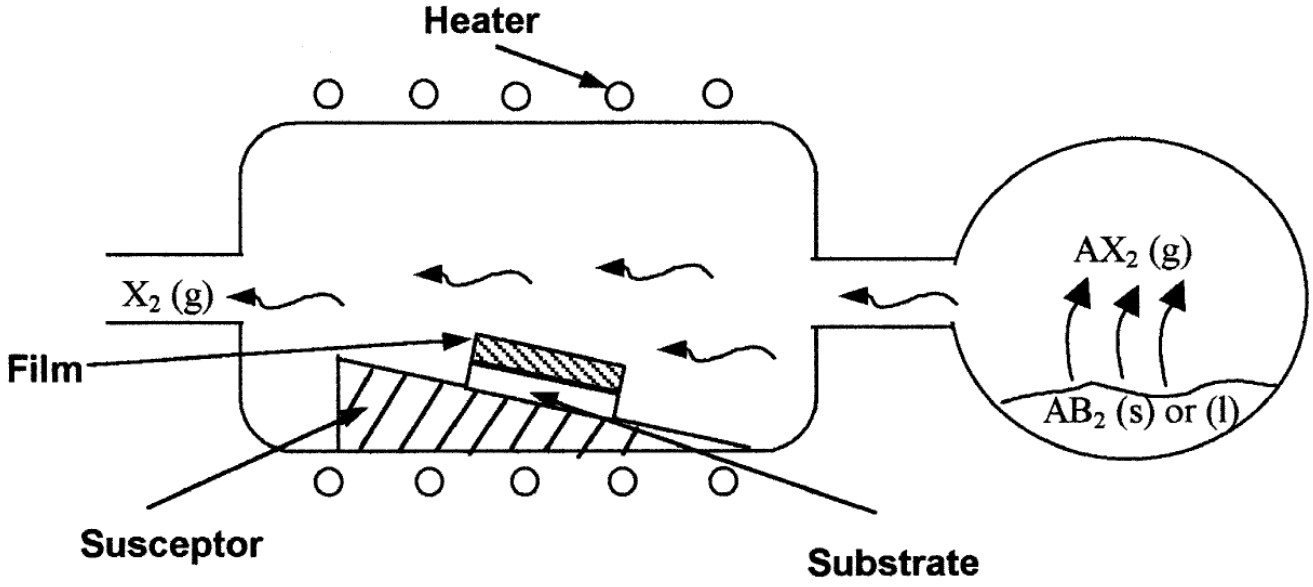

Precursors for CVD

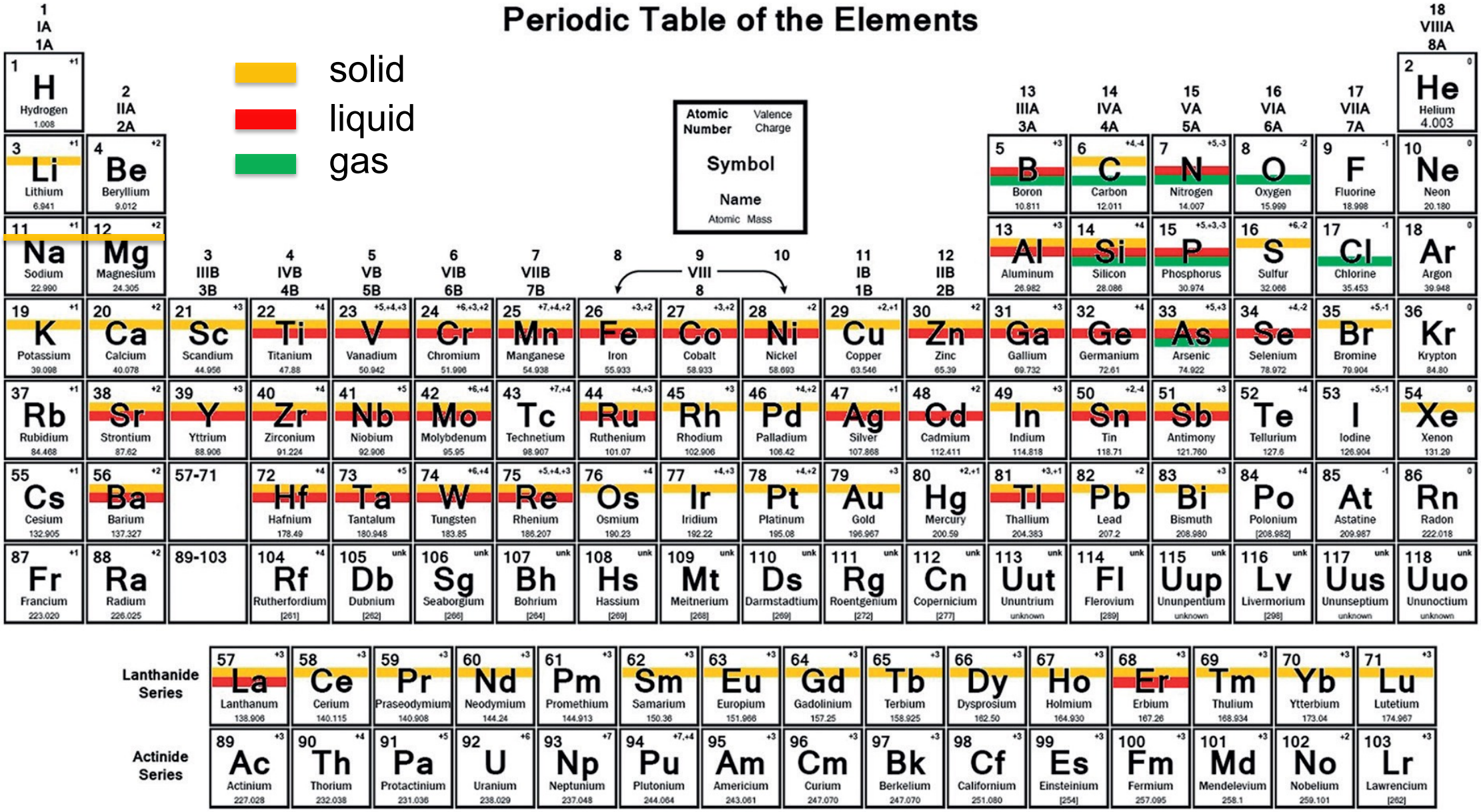

Metal-organic precursors

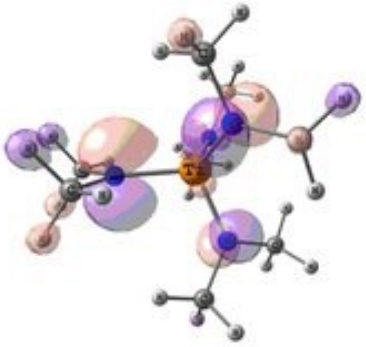

$Ti[N(CH_3)_2]_4$

(alkylamide)

$Ti[OCH(CH_3)_2]_4$

(alkoxide)

$Ti[(C_3H_7)N\text{-}C(CH_3)\text{-}N(C_3H_7)]_2$

(amidinate)

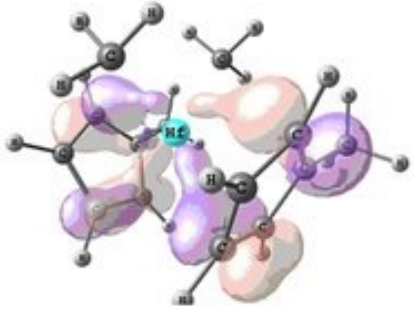

$[C_5H_5]_2Hf[CH_3]_2$

(cyclopentadienyl)

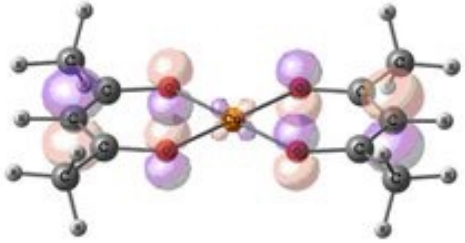

$Cu[CH_3\text{-}(CO)\text{-}CH\text{-}(CO)\text{-}CH_3]_2$

(diketonate)

$Al[CH_3CH_2]_3$

(alkyl)

J.C.F. Rodriguez-Reyes, Thesis 2010

- High purity and high yield
- Stability at ambient temperature
- Easiness to handle and non-toxicity
- Congruent volatilization with a significant temperature gap between evaporation and decomposition

Solid precursors

Thermogravimetric analysis (TG & DTG)

Good precursor

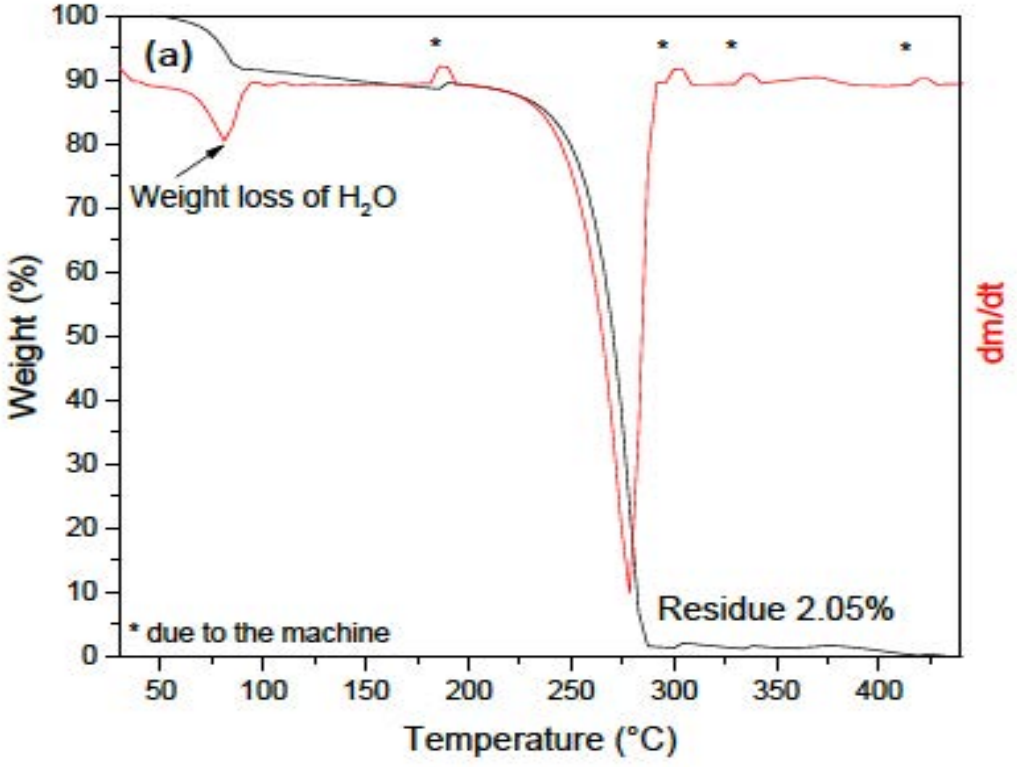

Bad precursor

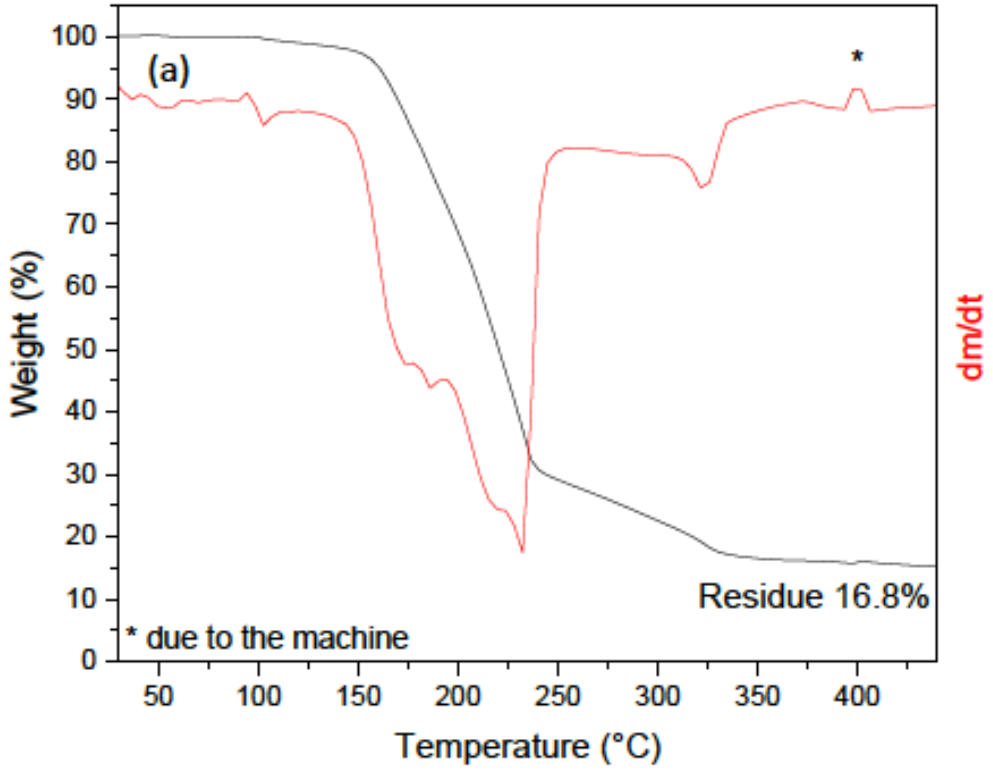

Solid precursors

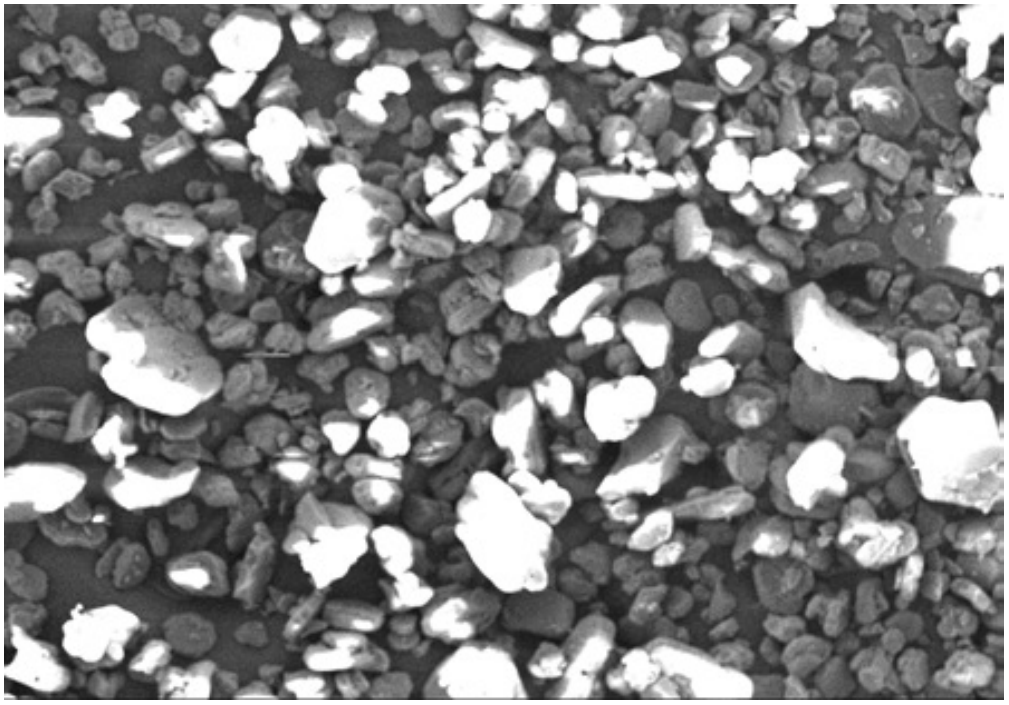

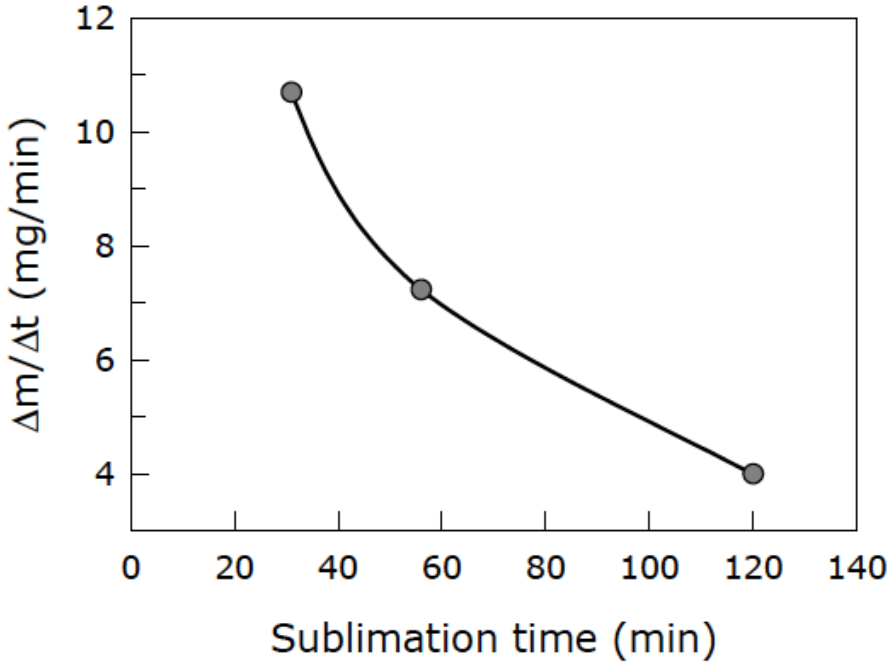

Dependence of evaporation rate:

- Surface area
- Time
- Degradation/aging

Vahlas et al. J. Electr. Soc. 2005

Irreproducibility

Solid precursors

Moving tape, powder injection

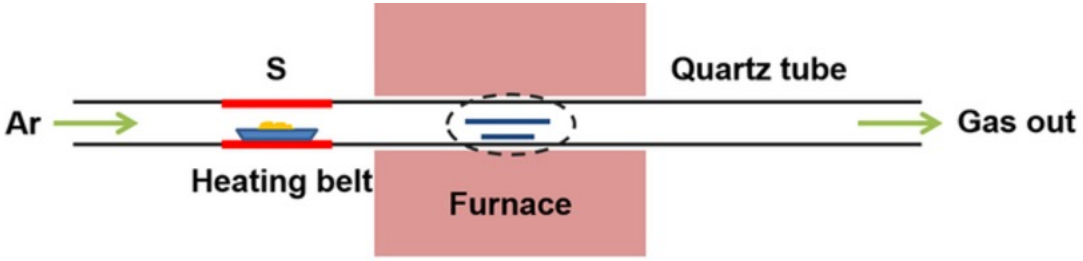

Lin et al. Scientific Reports 2015

Saturated stream

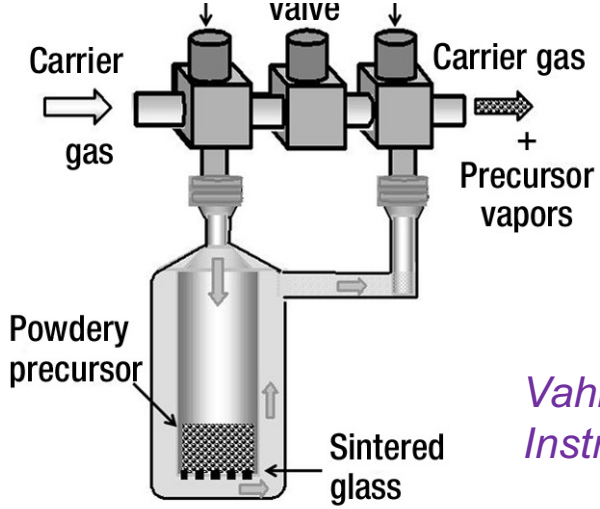

Vahlas et al. Gasses & Instrumentation 2009

Fluidized bed sublimation

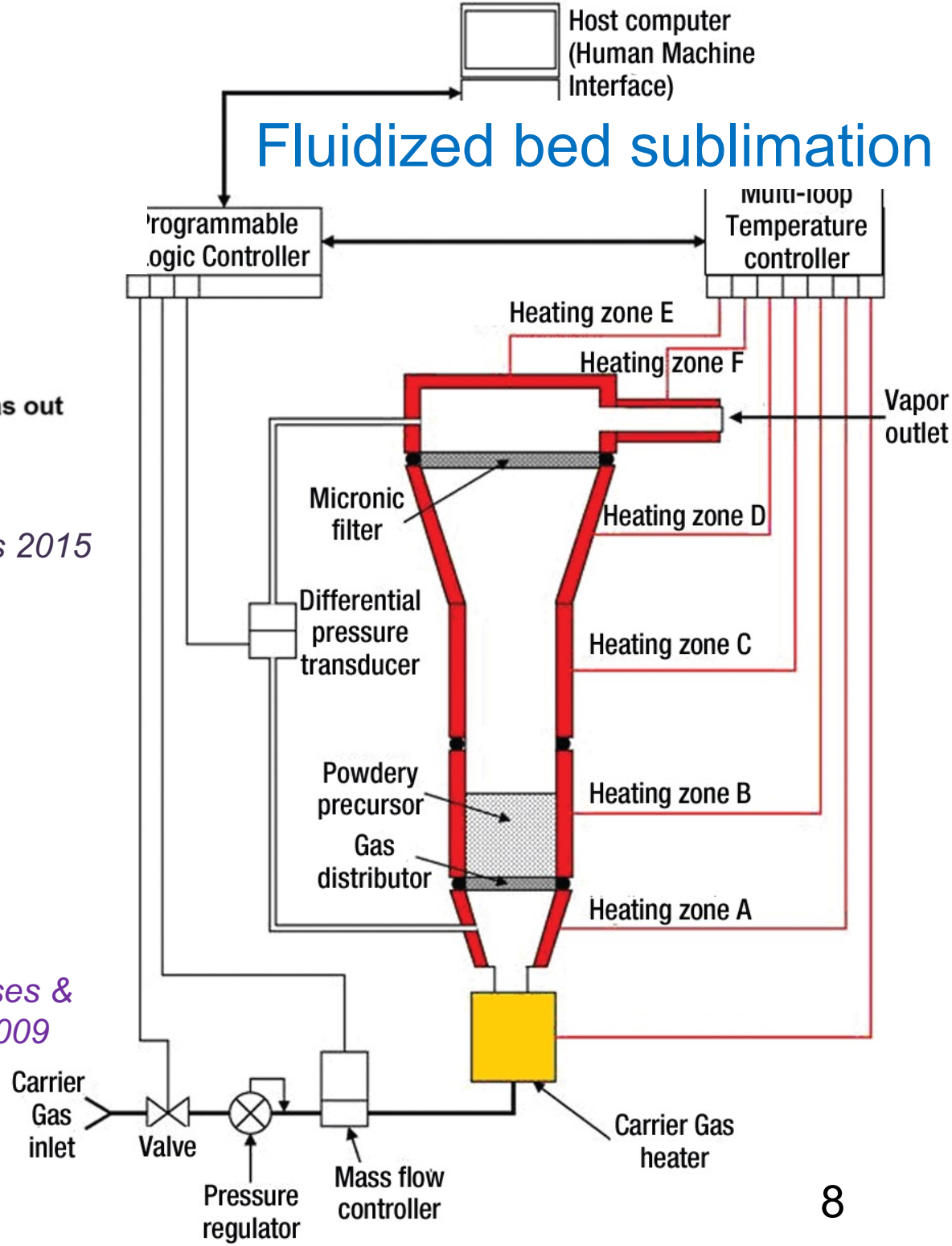

Solid precursors

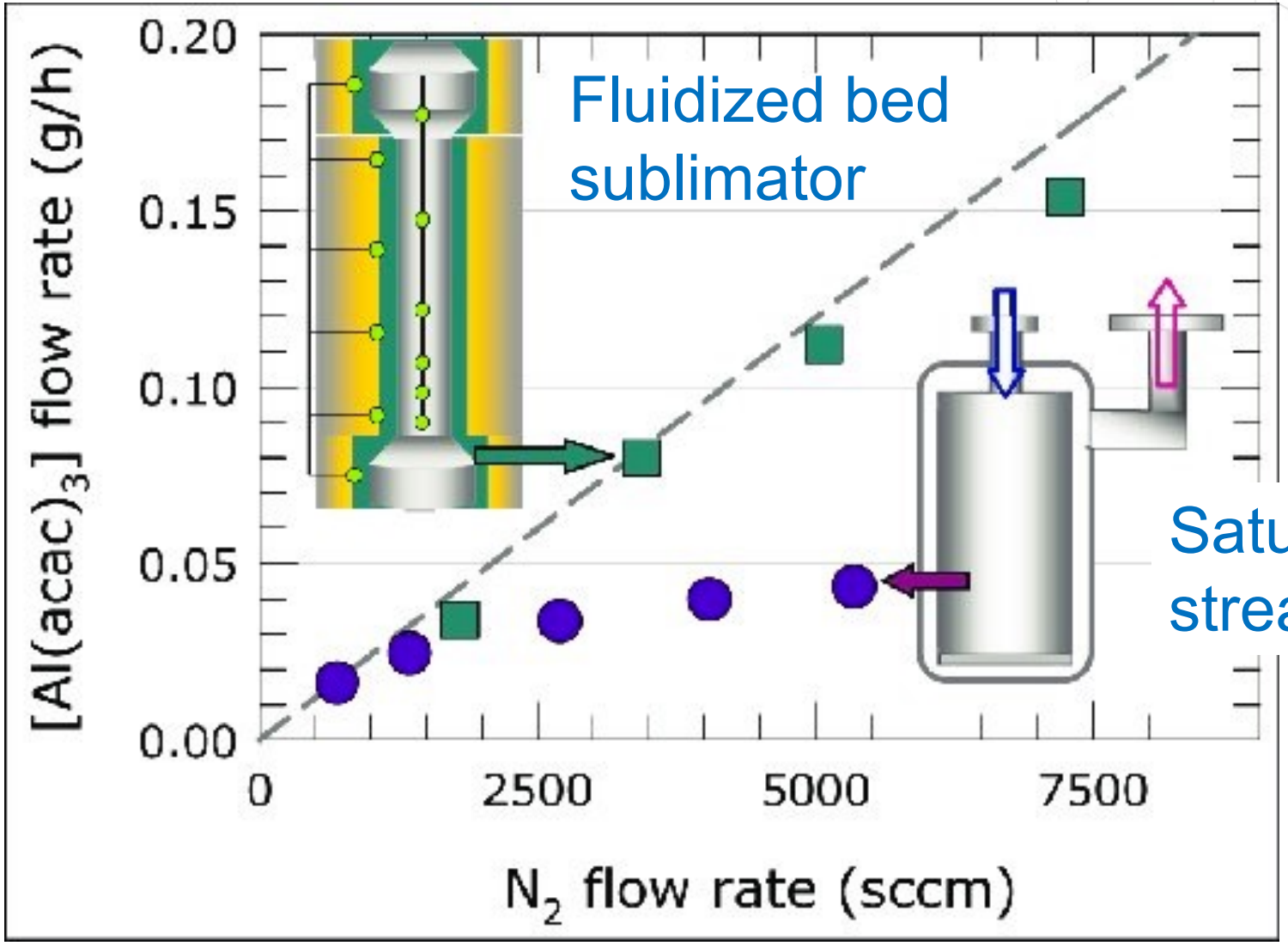

Vahlas et al. J. Electr. Soc. 2005

Liquid precursors/solutions

Bubbler

www.strem.com

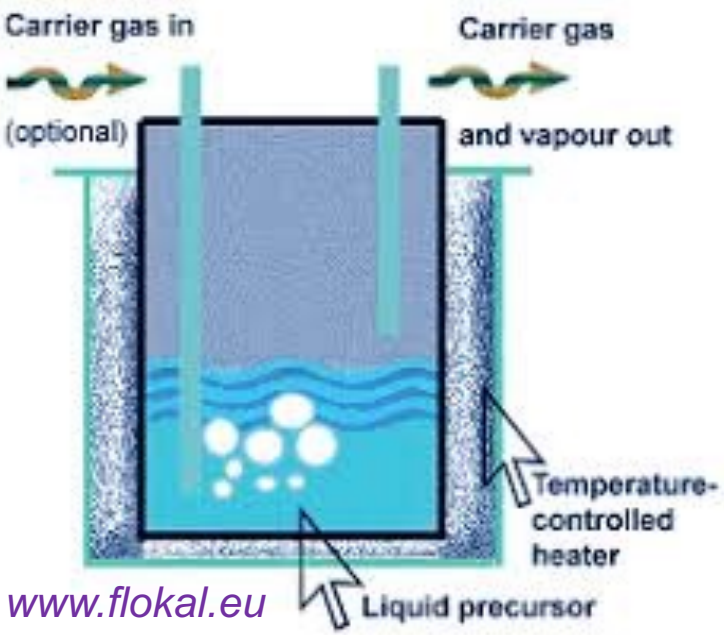

www.flokal.eu

Ultrasonic nozzle/ aerosol

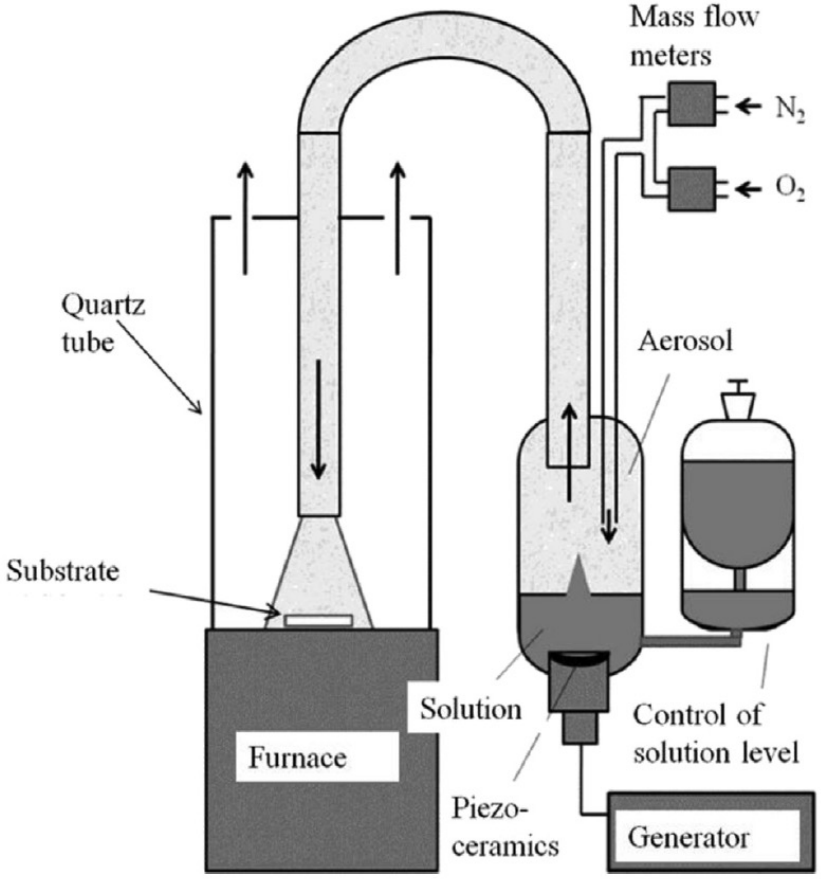

Bartasyte et al. J. Mat. Chem 2015

Capillary tubes & syringes

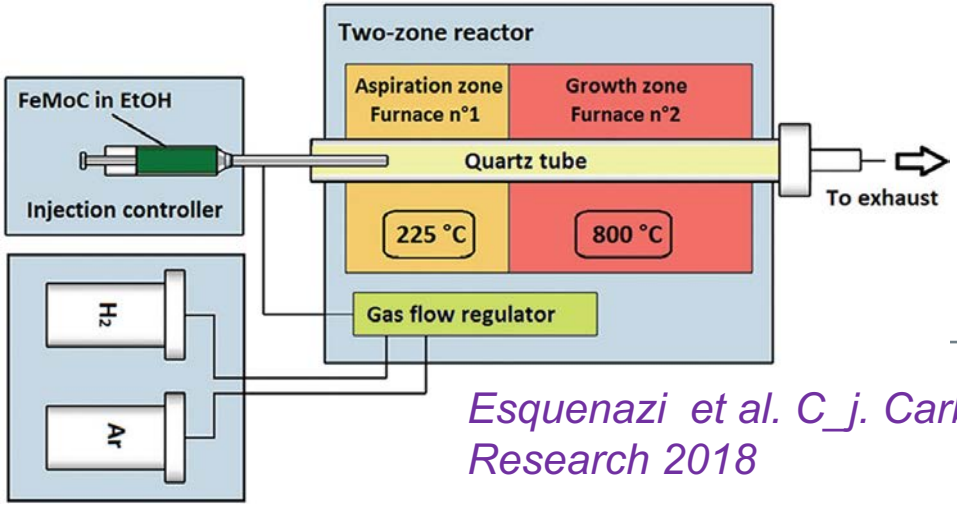

Esquenazi et al. C_j. Carbon Research 2018

Liquid precursors/solutions

Electrovalves

Senateur et al.
Patent no. 93/08838,
1993

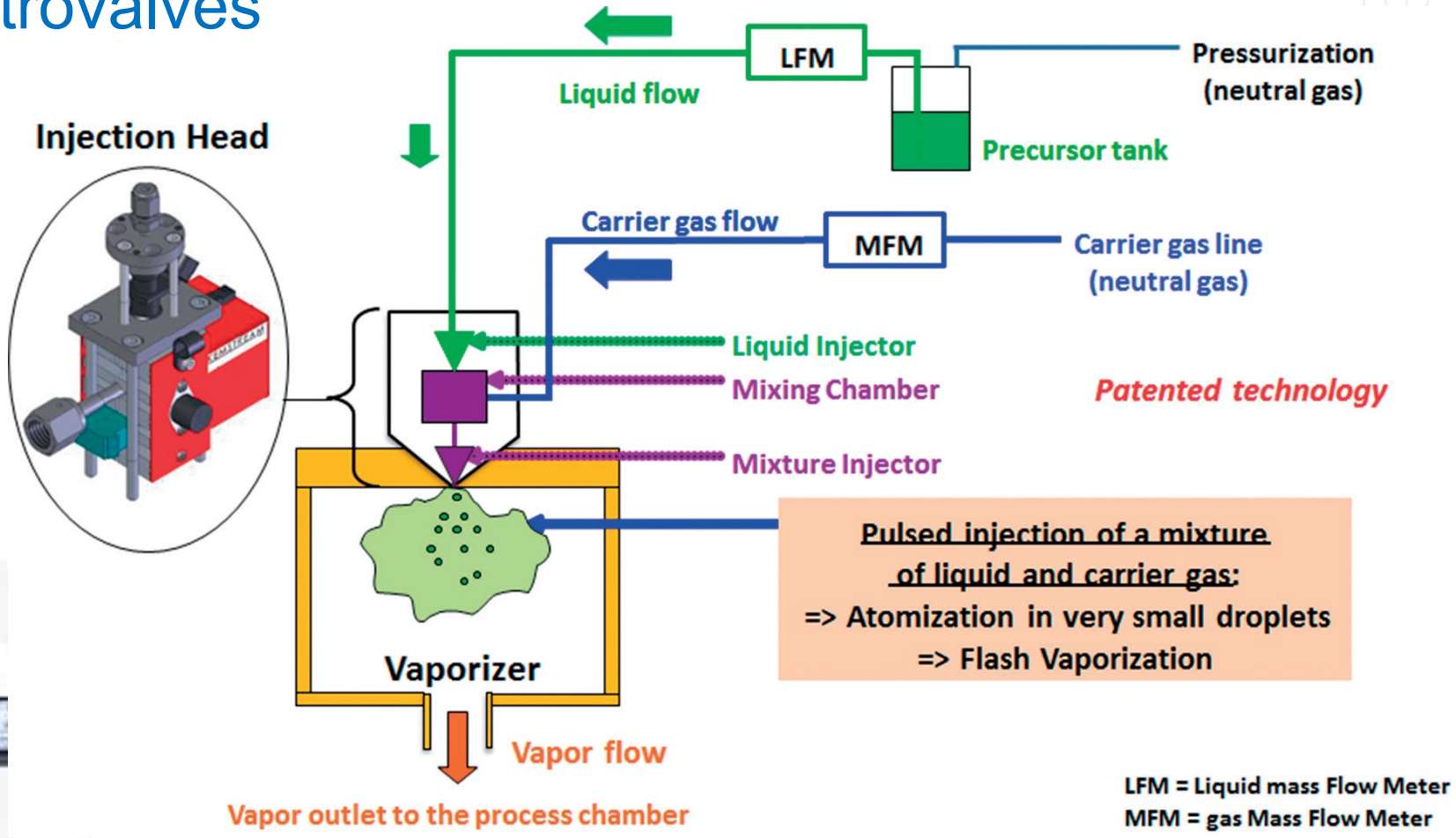

Liquid precursors/solutions

Electrovalves

- Special precise electromagn. valves-injectors,
- computer control (opening time and frequency)
- pulsed feeding of precursors (by micro-doses)
- flash evaporation
- "digital" growth of film
- solid & liquid MO precursors

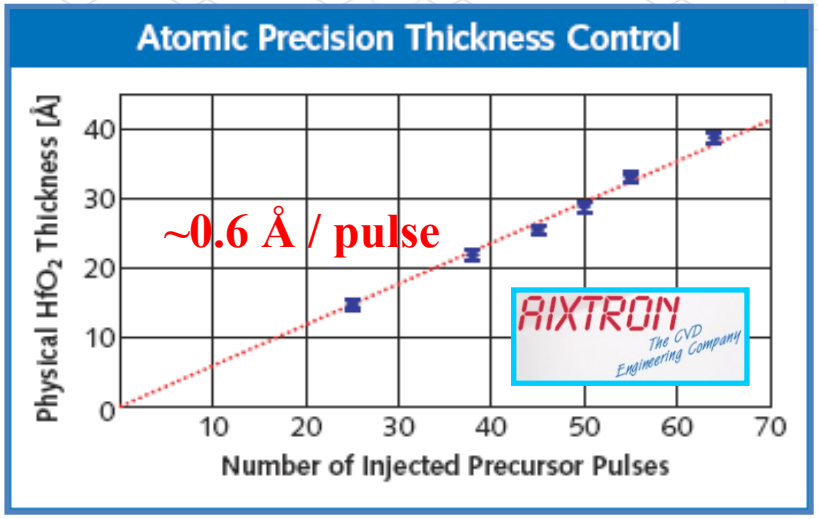

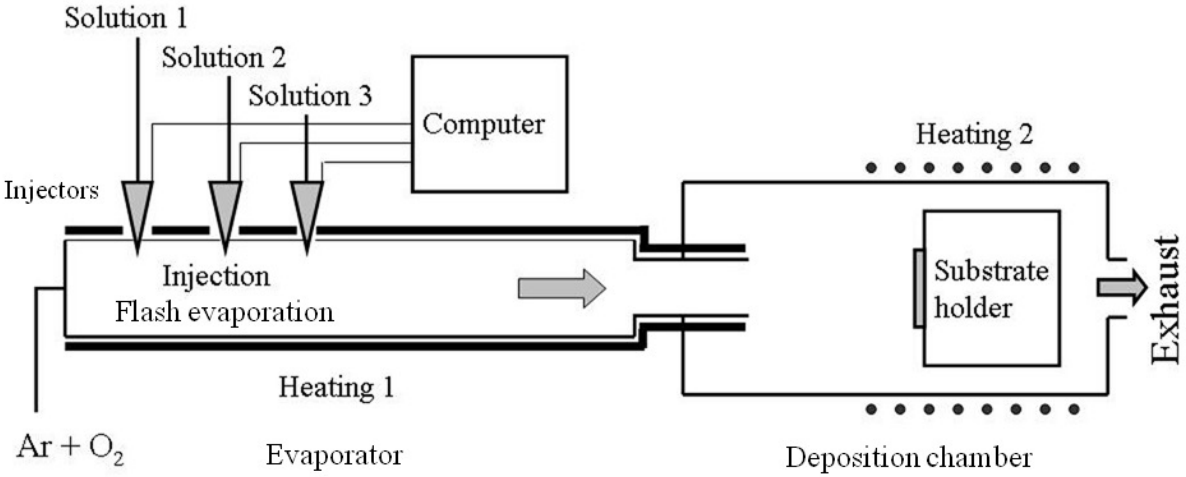

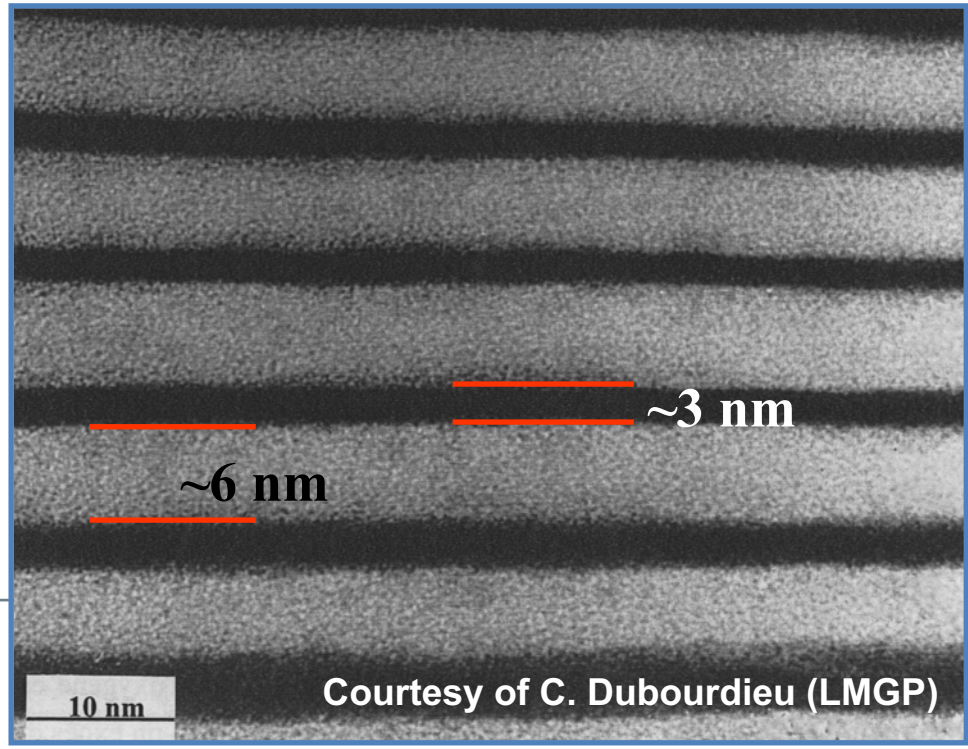

femto-st SCIENCES & TECHNOLOGIES

Temperature control in CVD reactor

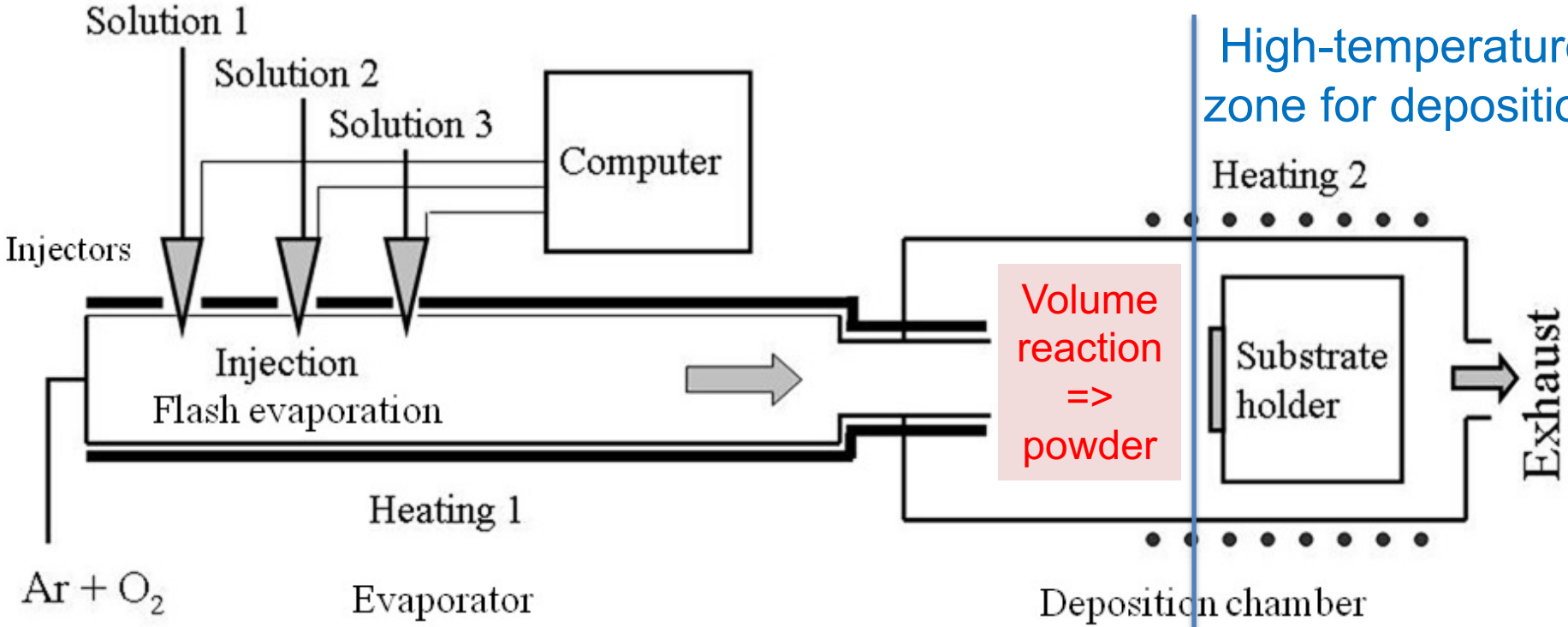

High-temperature zone for deposition

Optimise temperature to avoid condensation and premature decomposition of precurcors

Strong temperature gradient to favor surface reaction and to avoid volume reaction

Adsorption

Physical and chemical adsorption

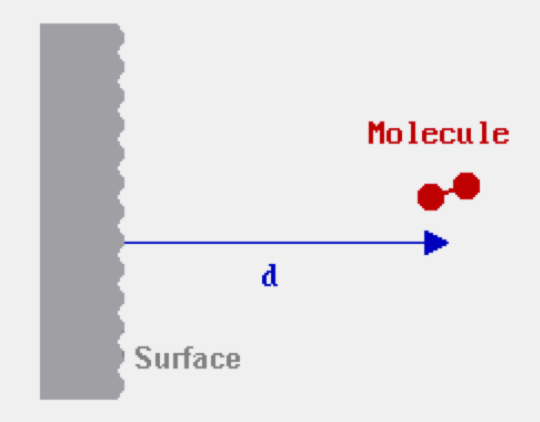

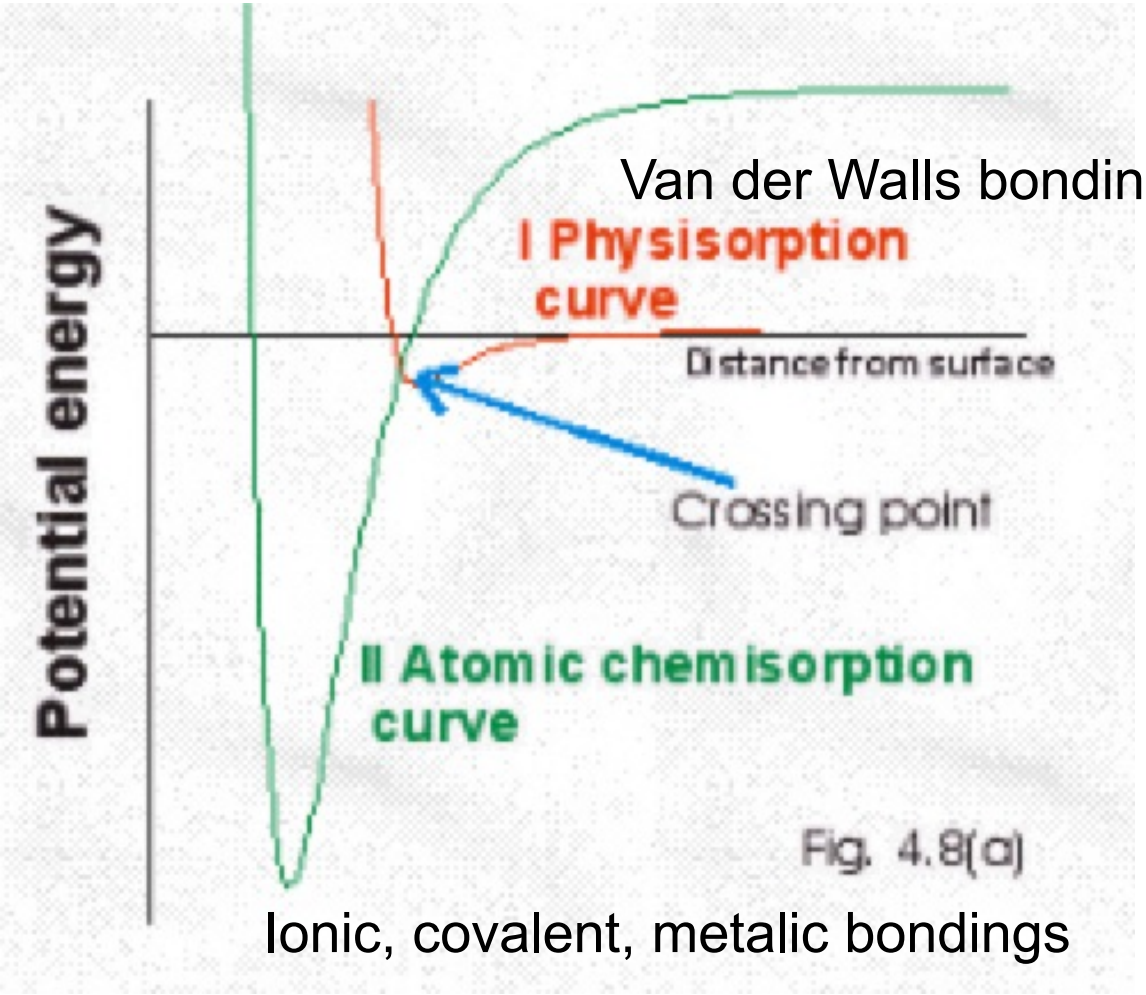

Van der Walls bondings

Ionic, covalent, metalic bondings

Adsorption

Physical and chemical adsorption

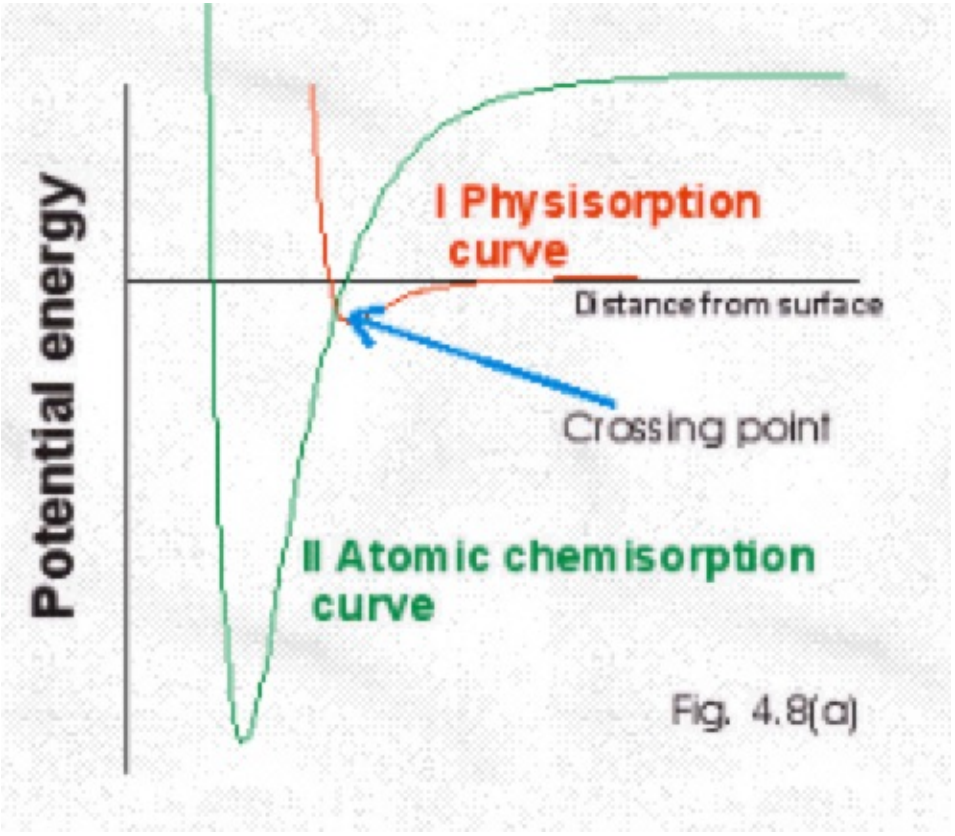

Maybe an issue for films grown at low temperature

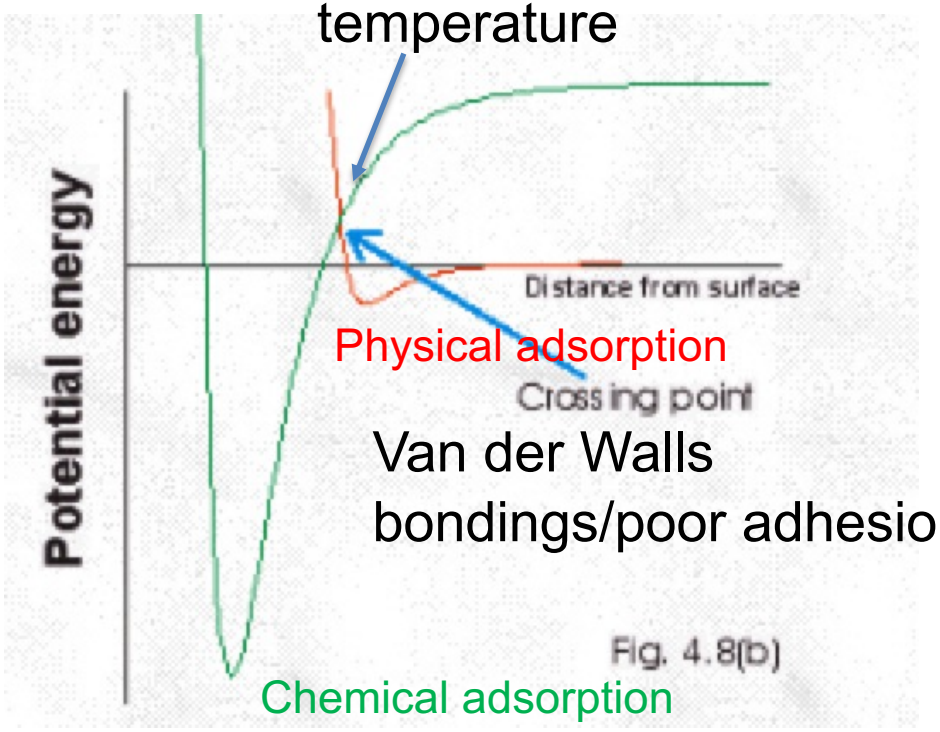

Van der Walls bondings/poor adhesion

Ionic, covalent, metallic bondings

Atomic Layer Deposition (ALD)

Absorption => Auto-limited surface reaction

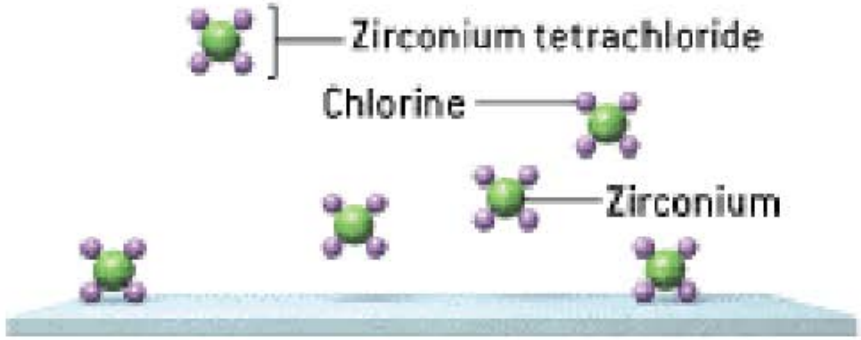

1 The surface is exposed to the first of two gases, here zirconium tetrachloride ($ZrCl_4$).

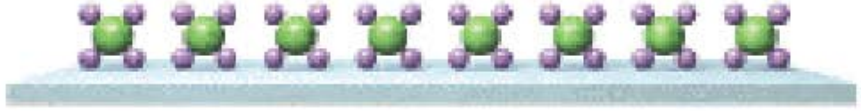

2 Molecules of $ZrCl_4$ adhere to the surface but not to one another.

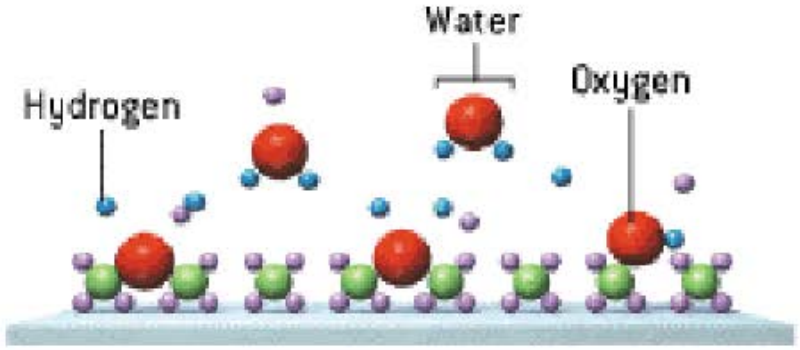

3 The coated surface is exposed to a second gas, in this case steam (H_2O).

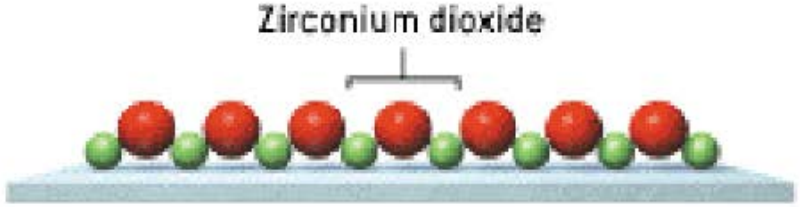

4 The $ZrCl_4$ on the surface reacts with the water (H_2O) to form a single-molecule-thick veneer of the desired material, zirconium dioxide (ZrO_2).

No reaction with the substrate

Adhesion

Adhesion « Rules »

Good aadhesion if

- Materials A and B forms solid solutions (phase diagrams), the bonding strenght of A-A, A-B, B-B are similar.
- semiconductor on semiconductor (IV, or III-V) with covalent bondings, metal on metal, oxide on oxide, nitride on nitride…

- Dirty surface may limit the adhesion (dust, layer…)

- Surface defects ameliorate adhesion (rough films)

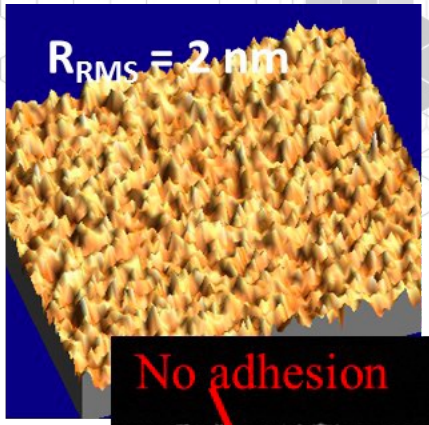

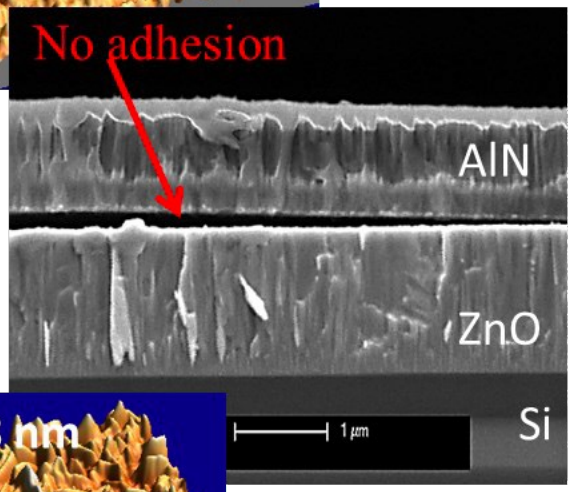

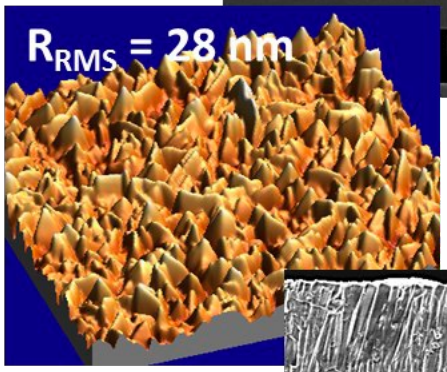

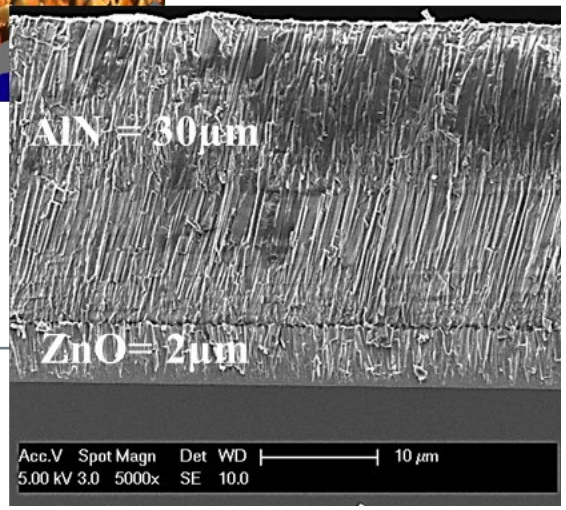

Good adherence AlN/ZnO

femto-st SCIENCES & TECHNOLOGIES

Chemical reactions

A. Pyrolysis (decomposition)

$SiH_4\ (g) \rightarrow \mathbf{Si(s)} + 2H_2\ (g)$ **(650°C)** Amorphous layers

B. Reduction (by H_2 or other reductors…)

$SiCl_4\ (g) + 2H_2(g) \rightarrow \mathbf{Si\ (s)} + 4HCl\ (g)$ **(1200°C)** Crystalline layers

C. Oxidation (by O_2, O_3, etc.)

$SiH_4\ (g) + O_2\ (g) \rightarrow \mathbf{SiO_2\ (s)} + 2H_2\ (g)$ **(450°C)**

D. Formation of compounds (carbides, nitrides, oxides, etc.)

$SiCl_4\ (g) + CH_4\ (g) \rightarrow \mathbf{SiC\ (s)} + 4HCl\ (g)$ **(1400°C)**

Chemical reactions

E. Formation of compounds (carbides, nitrides, oxides, etc.)

CVD organometalic precursors (OMCVD)

$$(CH_3)_3Ga\ (g) + AsH_3\ (g) \rightarrow \mathbf{GaAs\ (s)} + 3CH_4\ (g)$$

CVD metal-organic precursors (MOCVD)

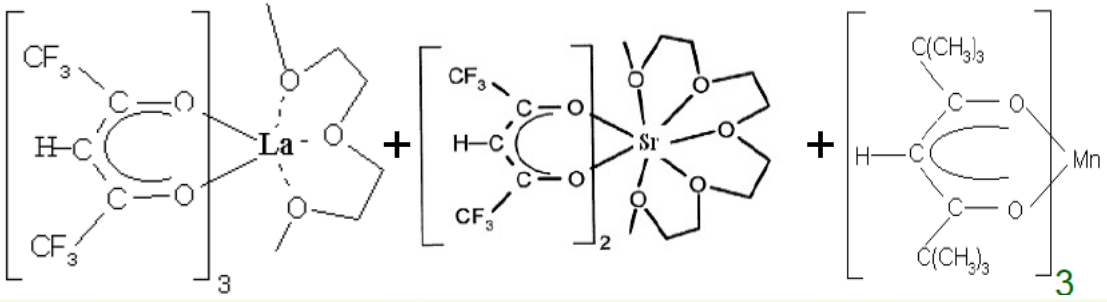

T_{dep}=850-950 ° C

$+ O_2 \longrightarrow La_{1-x}Sr_xMnO_3(s) + X(g) + Y(g) + \ldots$

Magnetoresistif materials
$La_{1-x}Sr_xMnO_3$

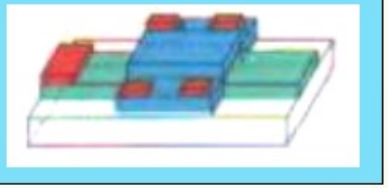

Superconductors
$YBa_2Cu_3O_{7-x}$ & $SmBa_2Cu_3O_{7-x}$

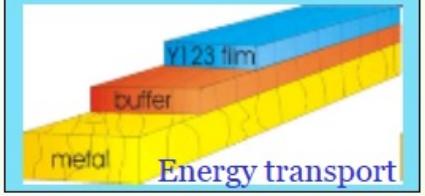

Mixed conducting oxides
$La_{1-x}(Sr,Ca)_xMnO_3$,
$La_{1-x}Sr_xFe_{1-y}Co_yO_3$,
$La_{1-x}Sr_xGa_{1-y}(Co, Ni, Fe)_yO_3$

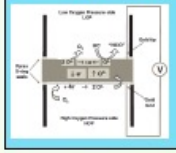

High-k dielectrics
Pr_2O_3, Pr_6O_{11}, Al_2O_3
$SrTiO_3$, YSZ

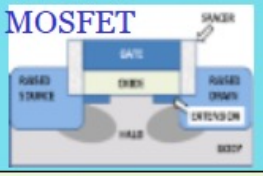

Ferroelectrics/ Piezoelectrics
$PbTiO_3/ZnO/LiNbO_3$
$LiTaO_3/KNbO_3$

femto-st SCIENCES & TECHNOLOGIES

Chemical reactions

A. Volume (homogeneous gas phase) reaction
=> Powder synthesis

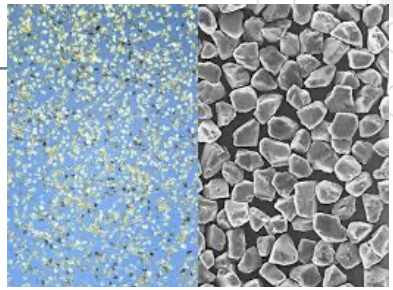

www.firstnano.com

B+A => Nanocomposites

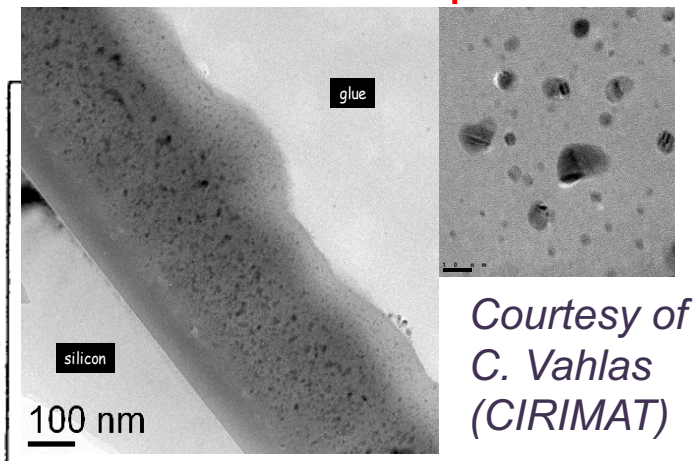

Courtesy of C. Vahlas (CIRIMAT)

A+B=> Nanocomposites

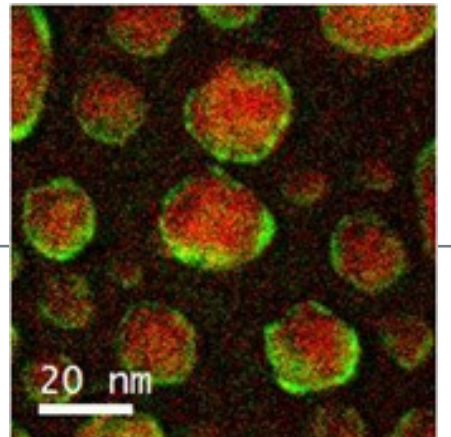

Courtesy of C. Vahlas (CIRIMAT)

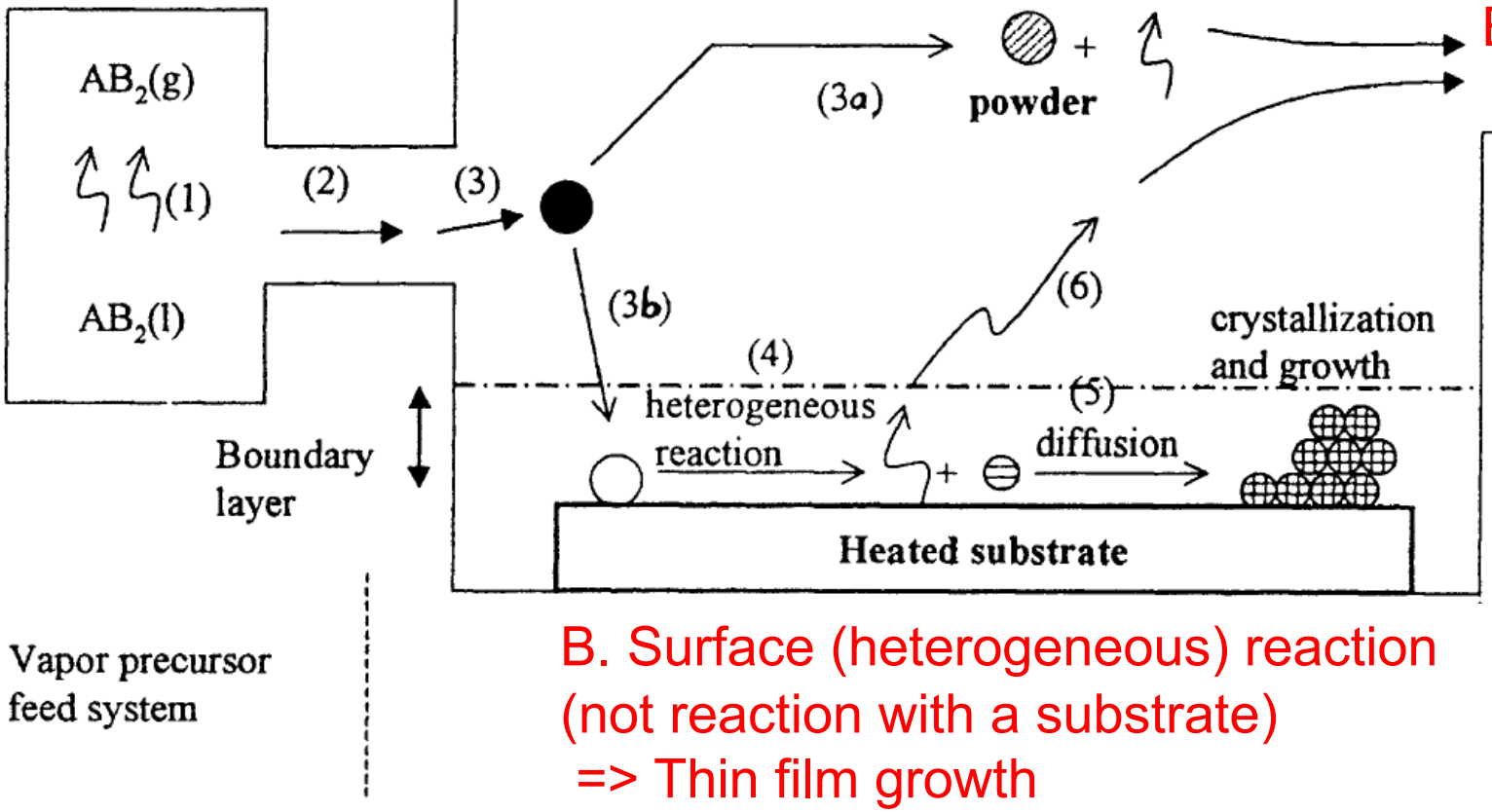

B. Surface (heterogeneous) reaction (not reaction with a substrate)
=> Thin film growth

Film growth from vapor phase

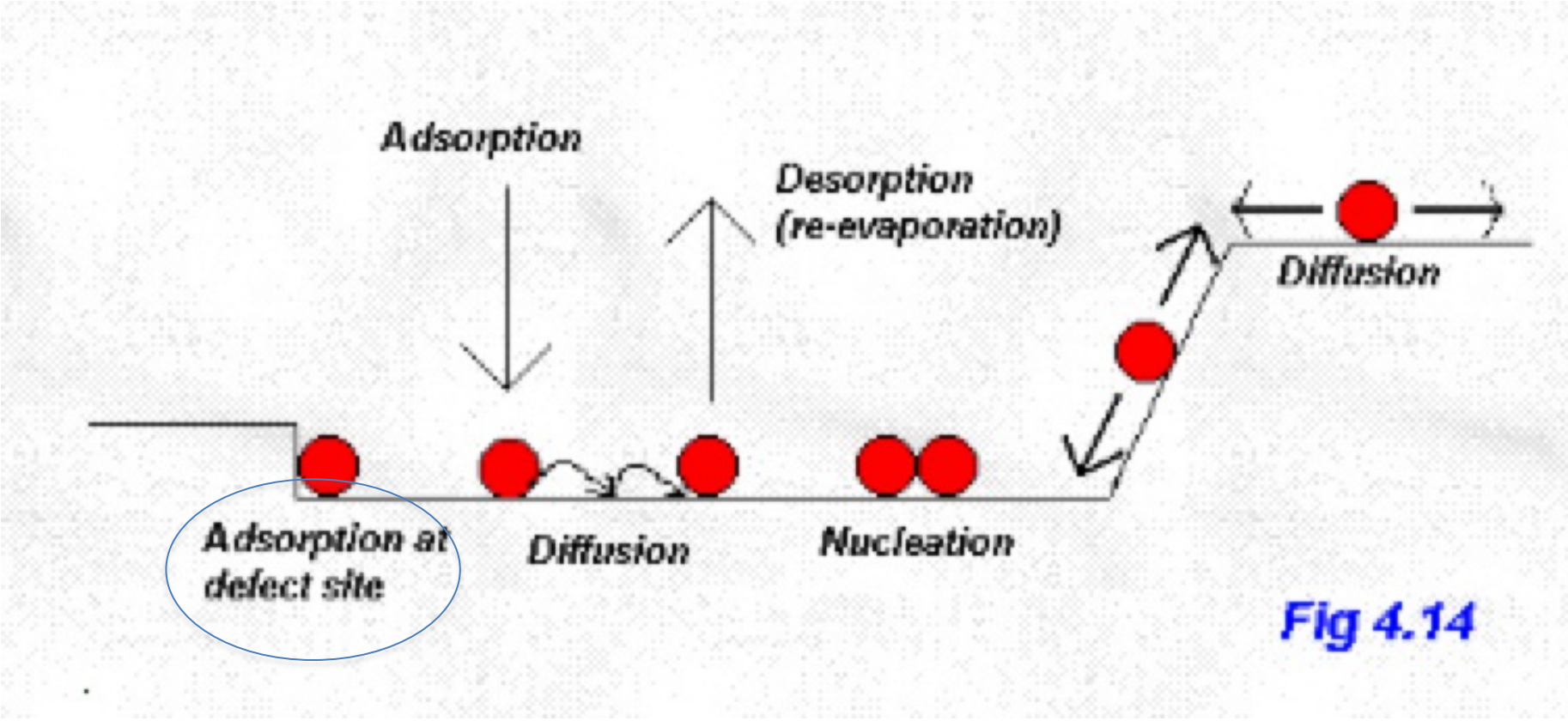

Diffusion

Atom can diffuse on the surface

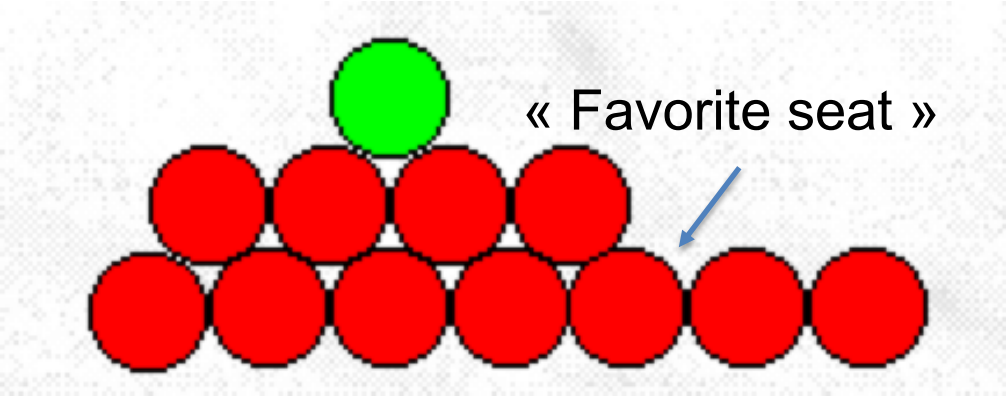

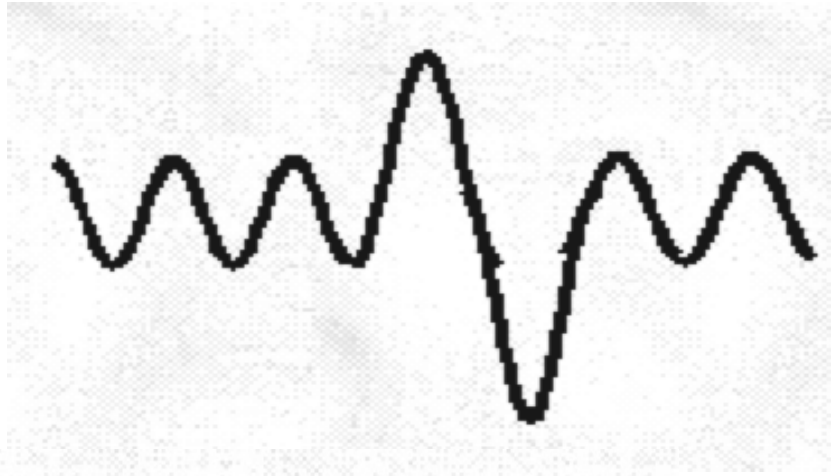

$$\nu_{diff} = \nu_{0(diff)} \exp(-E_{diff}/kT)$$

Atom diffusion rate highly dependent on:

- Temperature
- Surface quality/exposure
- Strength of bondings

Tammann's rule

$T_{Tammann}=0.52*T_{melting}$ (volume diffusion)

33% of $T_{melting}$ (for metals)
57% of $T_{melting}$ (for ionic crystals)
90% of $T_{melting}$ (for covalent crystals)

$T_{Hutting}=0.26*T_{melting}$ (surface/film)

Nucleation and growth of thin films

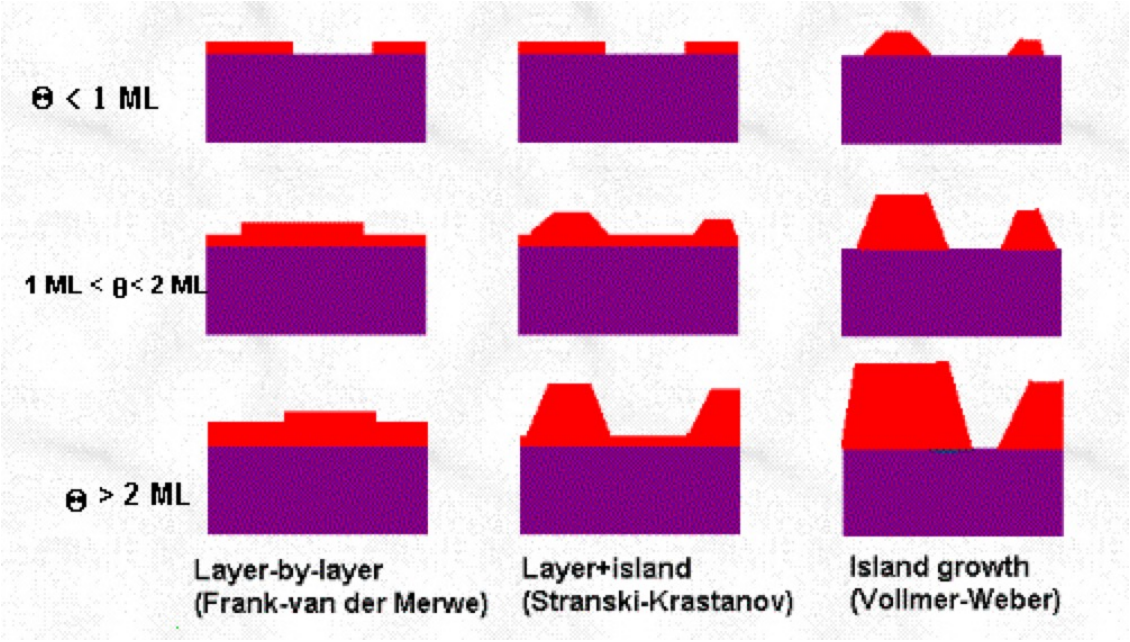

$$\Delta\gamma = \gamma_A + \gamma_I - \gamma_S$$

Film surface

Interface energy

Substrate surface

1. Mode « layer by layer»: $\Delta\gamma$ < 0
2. Mode « Island growth»: $\Delta\gamma$ >0
3. Mode « layer-island »: γ_I increases with thickness (lattice mismatch)

Island growth

Growth of Ag on NaCl (111)

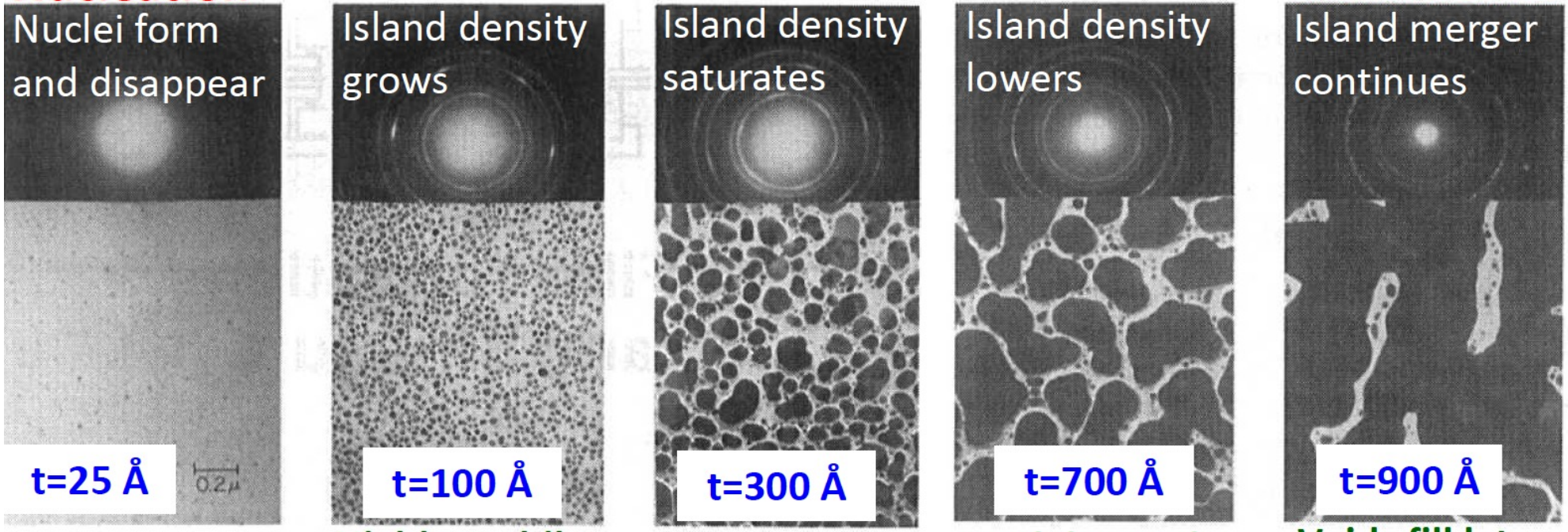

Grain size

Increase of deposition temperature:

- Increase of critical size of nucleus (grains)
- Longer formation time of continuous layer
- Higher critical thickness of continuous layer/ increased roughness

Increase of deposition rate:

- Smaller nucleus (grains)
- Lower thickness of continuous layer formation

Rough/poor quality substrate surface => small grains

Amorphous films => no grains

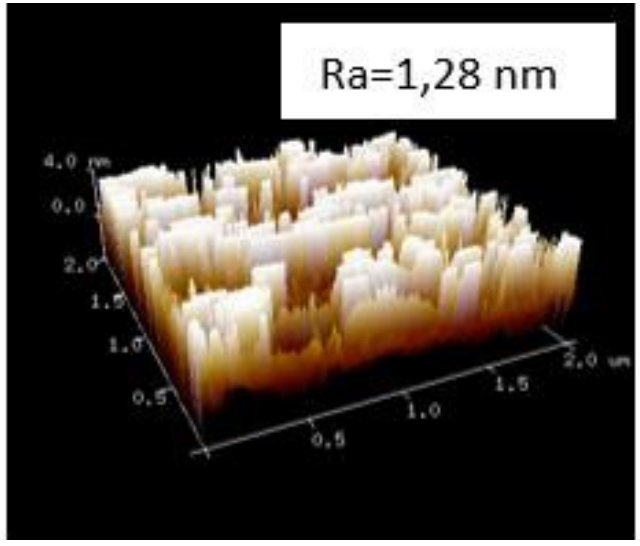

Kinetics & homogeneity

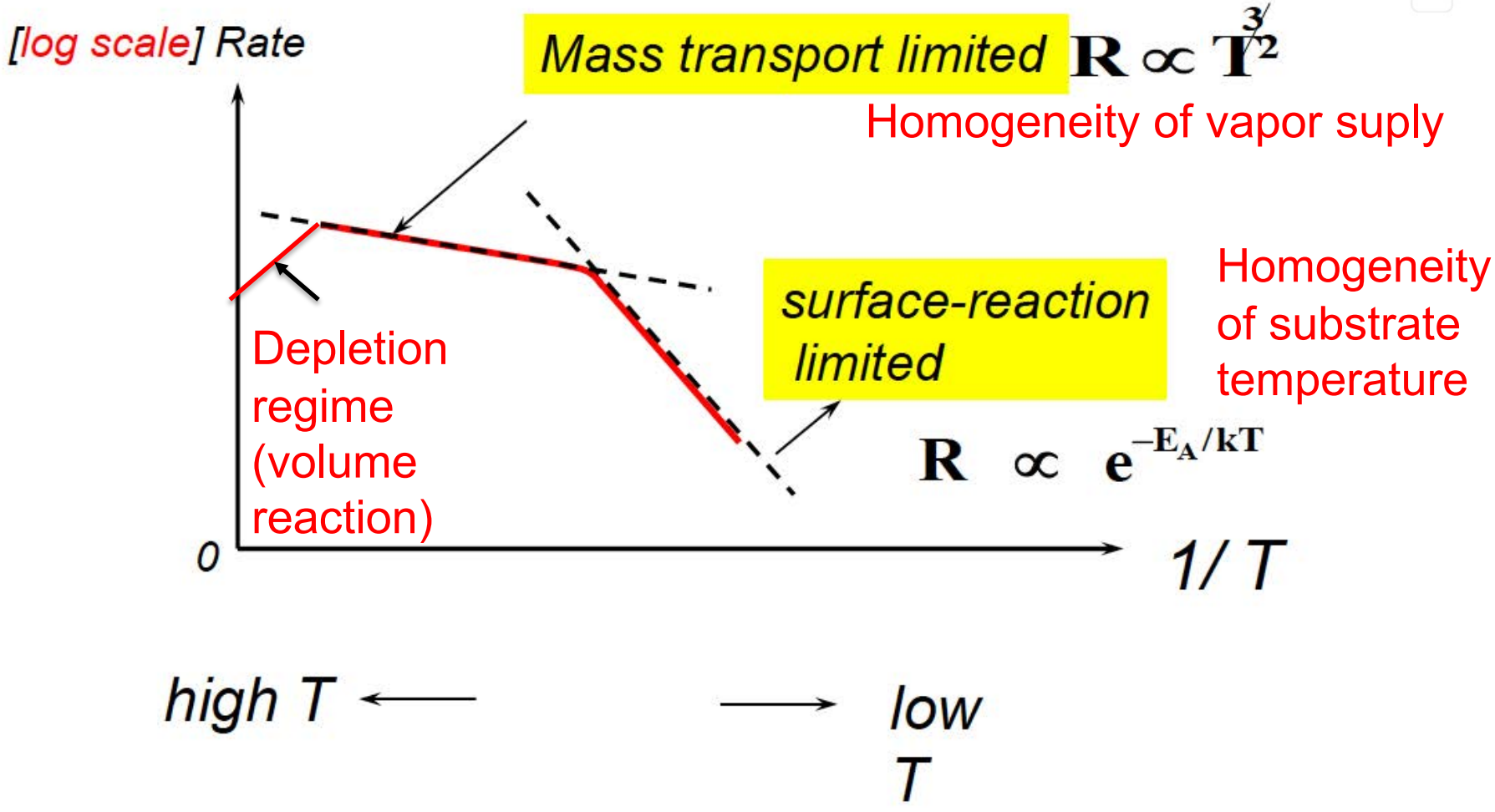

Asisted CVD (plasma, UV, laser e

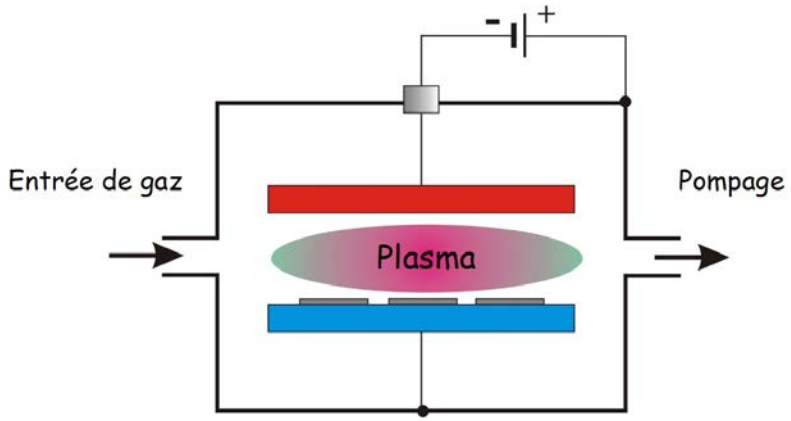

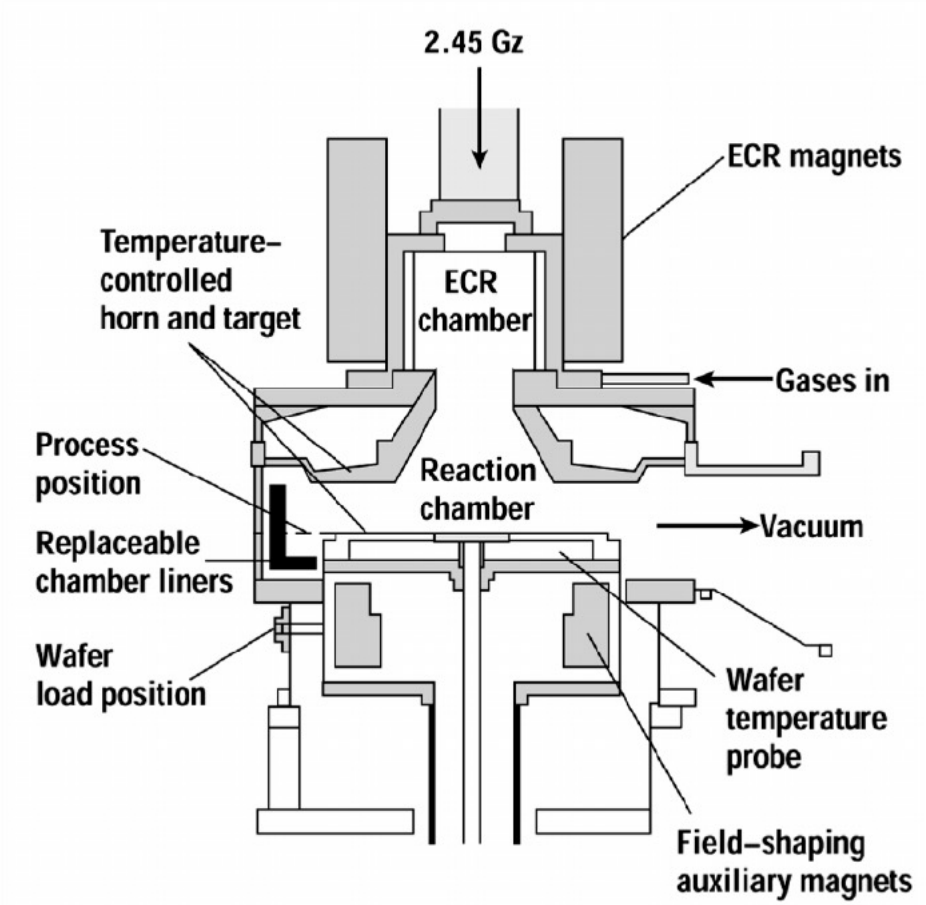

To decrease the deposition temperature

DIELECTRIC DEPOSITION PROCESSES

	Deposition Temperature	
	LPCVD	PECVD
$SiH_4 + NH_3 \Rightarrow Si_3N_4$	850° C	200-400°C
$SiH_4 + N_2O \Rightarrow SiO_2$	800°C	200-400°C
$TEOS + O_2 \Rightarrow SiO_2$	720°C	350°C
$SiH_4 + O_2 \Rightarrow SiO_2$	400°C	

Conformity

CVD: AR < 10

ALD: AR < 100

Not valid for plasma assisted processes

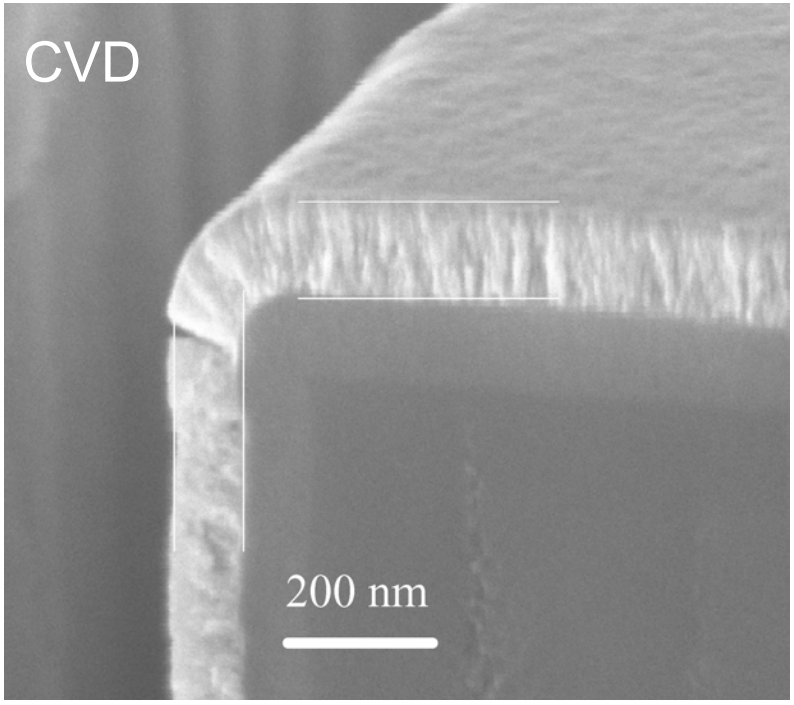

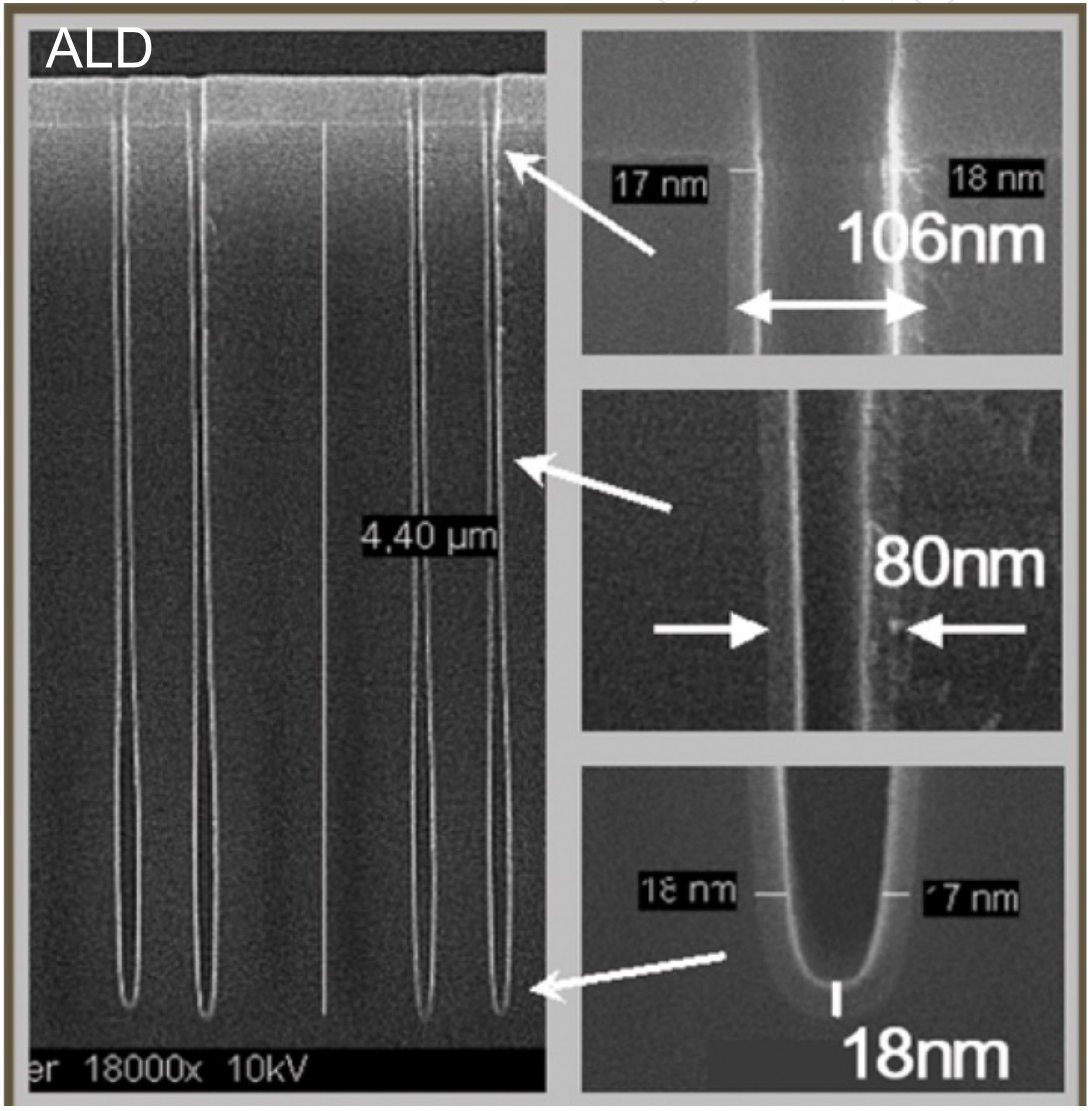

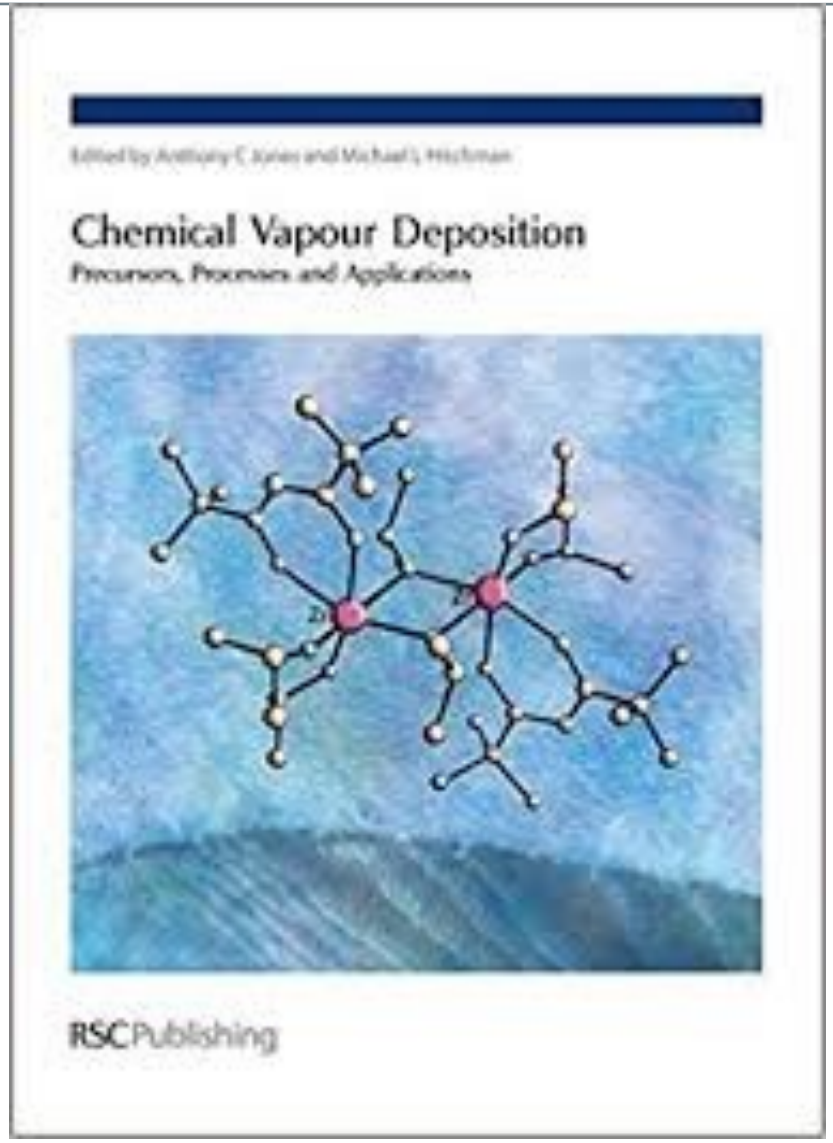

And many other books!

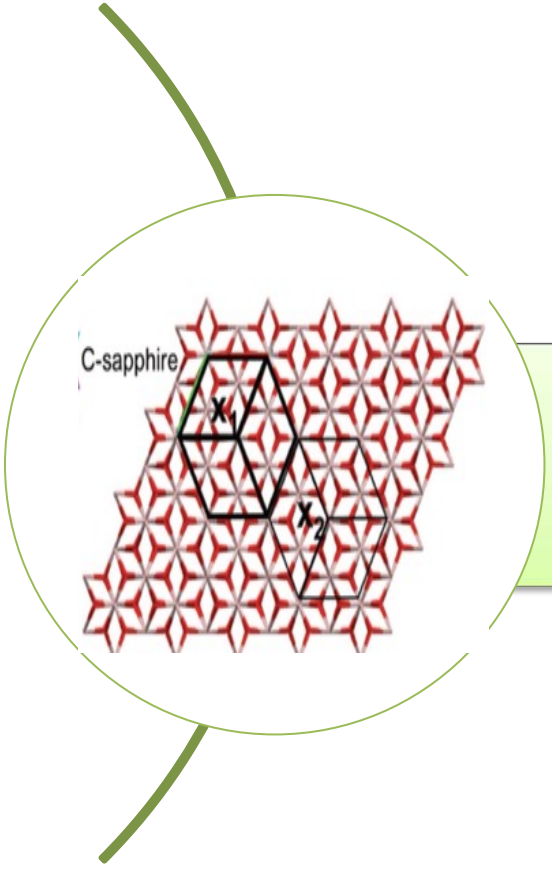

Structure & Orientation

Thin films

Temperature/energy is high enough to crystallize

Temperature/energy too low to crystallise

Tensors

Tensor rank	Tensor transformation	Geometrical representation	Property relating	Examples of physical properties
0 (scalar)	$A'=A$	sphere	Two scalars	Heat capacity Volume density
1 (vector)	$A_i'=a_{ij}A_j$ $A_j=a_{ij}A_i'$	vector	Scalar and vector	Pyroelectricity Electrocaloric effect
2	$A_{ij}'=a_{im}a_{jn}A_{mn}$ $A_{mn}=a_{im}a_{jn}$ A_{ij}'	quadric	Two vectors	Permitivitty Electical conductivity Thermal conductivity
			Scalar and 2nd rank tensor	Thermal expansion Piezocaloric effect
3	$A_{ijk}'=a_{im}a_{jn}a_{ko}$ A_{mno} $A_{mno}=a_{im}a_{jn}a_{ko}A_{ijk}'$	cubic	Vector and 2nd rank tensor	Direct piezoelectric effect Converse piezoelectric effect Electro-optical effect
4	$A_{ijkl}'=a_{im}a_{jn}a_{ko}a_{lp}A_{mnop}$ $A_{mnop}=a_{im}a_{jn}a_{ko}a_{lp}A_{ijkl}'$	quartic	Two 2nd rank tensors	Elastic compliance Elastic stiffness Elasto-optical coefficients Piezo-optical coefficients Electrostriction

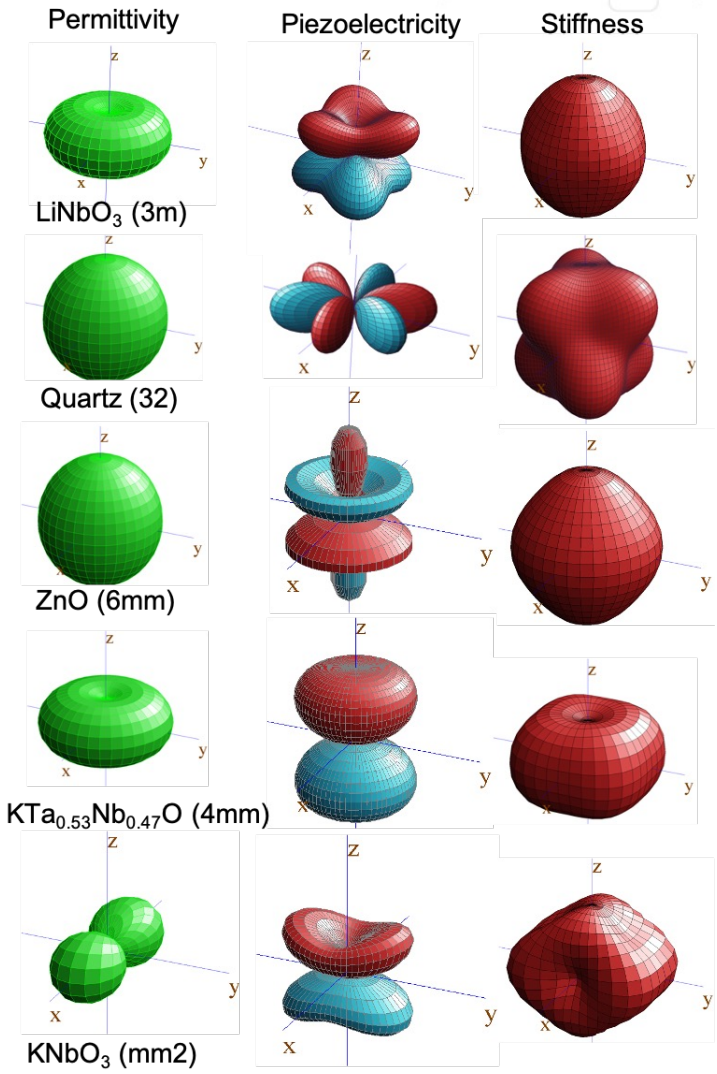

In amorphous films no 1st & 3rd rank properties

Ceramics, polycrystalline & textured materials

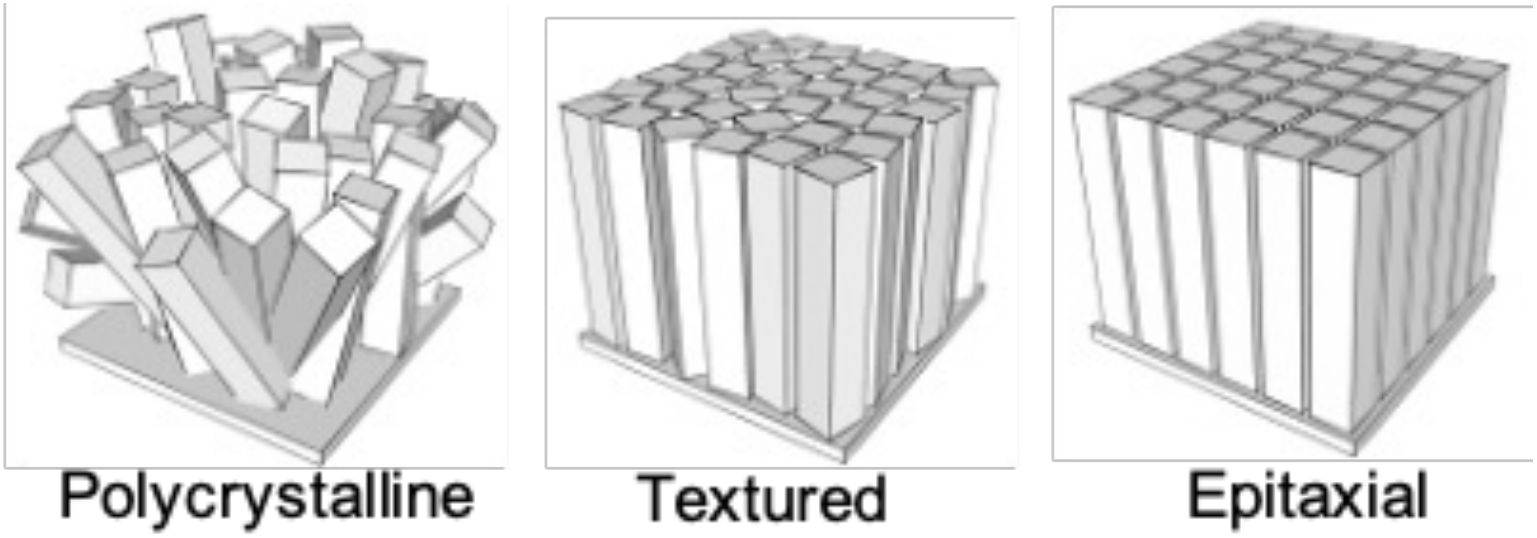

Textured film: film crystalline orientation is defined along growth axis but not in the substrate plane

Epitaxial films : in-plane orientation controlled by the substrate orientation (may contain growth domains and/or several coexisting epitaxial orientations)

Single crystalline layers: Single in-plane and out-of plane crystalline orientation (no growth domains)

Ceramics, polycrystalline & textured materials

Polycrystalline material

$$\langle K'_{11}\rangle = K_{11}\langle a_{11}^2\rangle + K_{22}\langle a_{12}^2\rangle + K_{33}\langle a_{13}^2\rangle$$

$$\langle a_{11}^2\rangle = \frac{\int_{-1}^{+1} a_{11}^2\,\mathrm{d}a_{11}}{\int_{-1}^{+1}\mathrm{d}a_{11}} = \frac{1}{3} = \langle a_{12}^2\rangle = \langle a_{13}^2\rangle.$$

$$\langle K'_{11}\rangle = \frac{1}{3}(K_{11} + K_{22} + K_{33}).$$

Macro properties are represented by averages
Each single crystallite remains anisotropic !
Ceramics are highly sensitive to thermal stresses!

PZT (lead zirconate titanate)

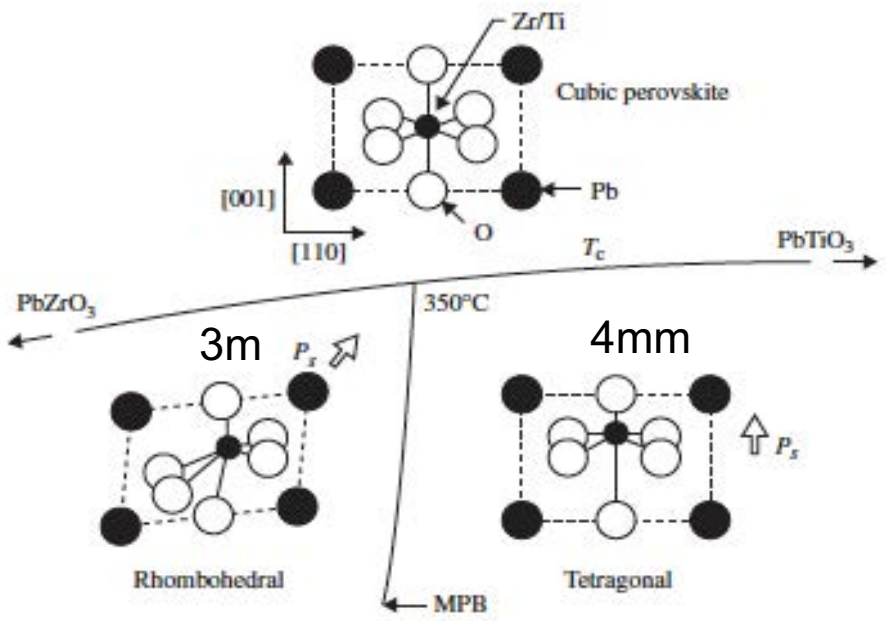

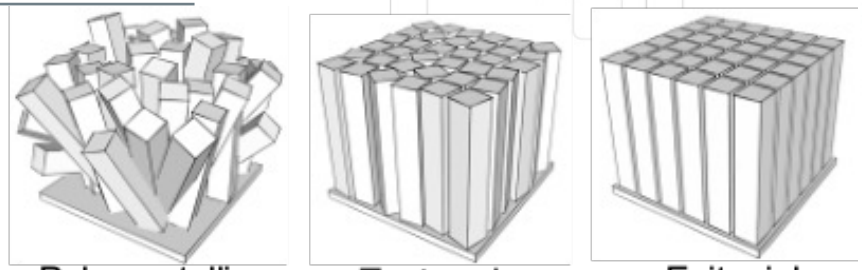

Polycrystalline (∞∞m) and unpoled textured (∞/mm) materials:

$$\begin{pmatrix} 0 & 0 & 0 & 0 & 0 & 0 \\ 0 & 0 & 0 & 0 & 0 & 0 \\ 0 & 0 & 0 & 0 & 0 & 0 \end{pmatrix}$$

3m point group (single crystals):

$$\begin{pmatrix} 0 & 0 & 0 & 0 & d_{15} & -2d_{22} \\ -d_{22} & d_{22} & 0 & d_{15} & 0 & 0 \\ d_{31} & d_{31} & d_{33} & 0 & 0 & 0 \end{pmatrix}$$

hexagonal cell with 3-fold axis II c-axis

4mm & ∞m point (poled textured materials) groups:

$$\begin{pmatrix} 0 & 0 & 0 & 0 & d_{15} & 0 \\ 0 & 0 & 0 & d_{15} & 0 & 0 \\ d_{31} & d_{31} & d_{33} & 0 & 0 & 0 \end{pmatrix}$$

Textured films

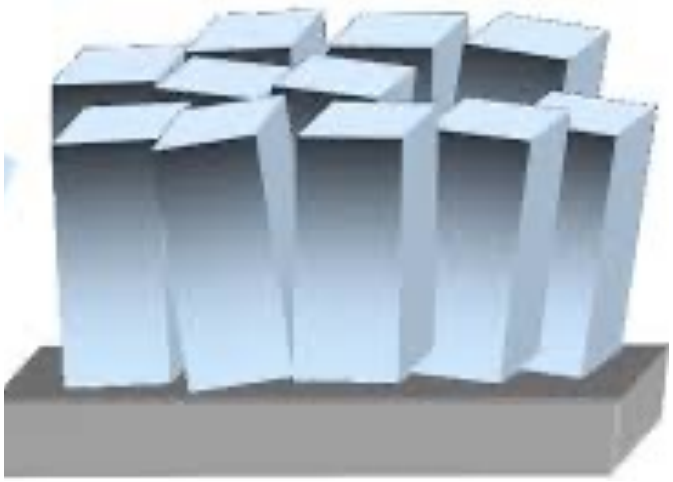

Textured film: film crystalline orientation is defined along growth axis but not in the substrate plane

Textured films grows oriented naturally by keeping lowest surface energy and this orientation is independent on the substrate nature

Textured films

- ***Pt surface energy***

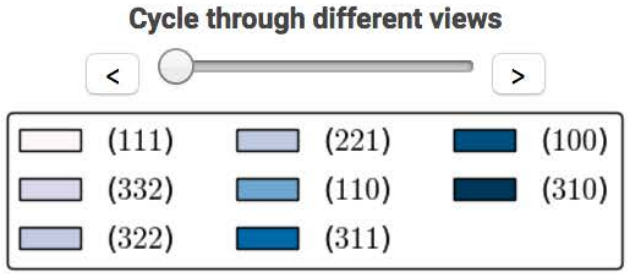

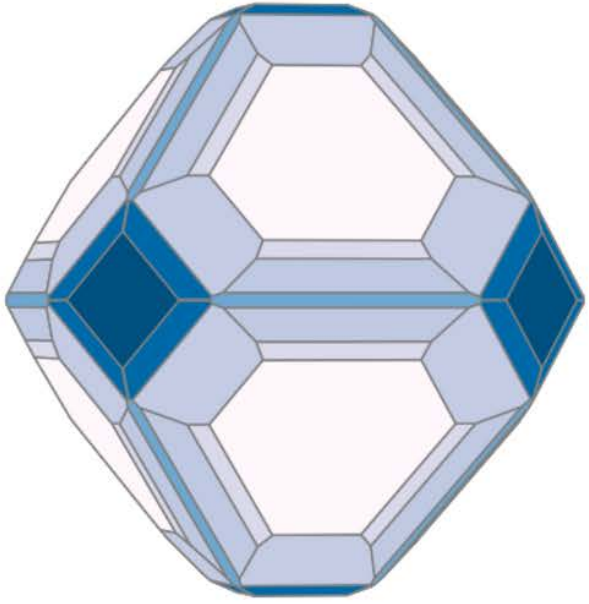

Miller indices	γ	
	J/m^2	eV/Å^2
(111)	1.48	0.092
(332)	1.56	0.097
(322)	1.59	0.099
(221)	1.60	0.100
(110)*	1.68	0.105
(331)	1.71	0.106
(211)	1.76	0.110
(321)	1.77	0.110
(311)	1.79	0.112
(100)	1.84	0.115
(110)	1.87	0.117

Singh-Miller & Marzari (MIT 2009)

Pattern : 04-001-0112 ***Radiation =*** 1.788970

Pt

Platinum
Platinum, syn

2th	i	h	k	l
46.523	999	1	1	1
54.261	461	2	0	0
80.318	238	2	2	0
98.265	243	3	1	1
104.344	67	2	2	2
131.578	30	4	0	0
167.310	95	3	3	1
	91	4	2	0
	80	4	2	2

Lattice : Face-centered cubic

S.G. : Fm-3m (225)

a = 3.92300

Mol. weight = 195.09

Volume [CD] = 60.37

Dx = 21.463

Thin films & nanowires

Dense planes = low surface energy

Growth rate

Polycrystalline/
epitaxial films

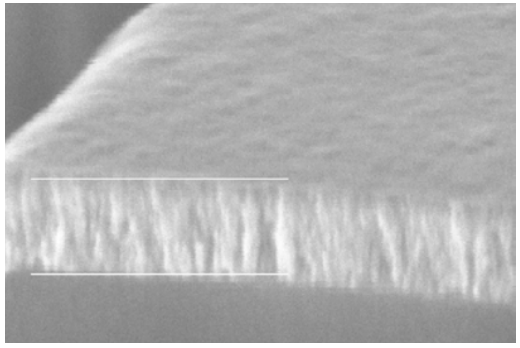

Textured films

Nanowires

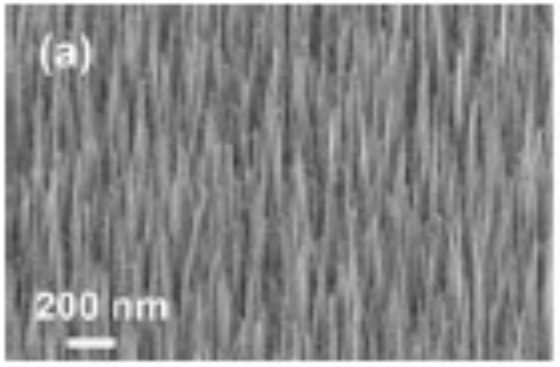

Nucleous density= nanowires density

Roughness

Other origins of roughness:
- Nanostructural growth
- Polycrystallinity/ differential growth of grains
- Big grains
- Stress

Solutions:
- Amorphous films
- Epitaxial films
- Decrease grain size by reducing surface mobility

  => Parameters: reduce temperature, increase pressure, or reduce growth rate for epitaxial/textured films

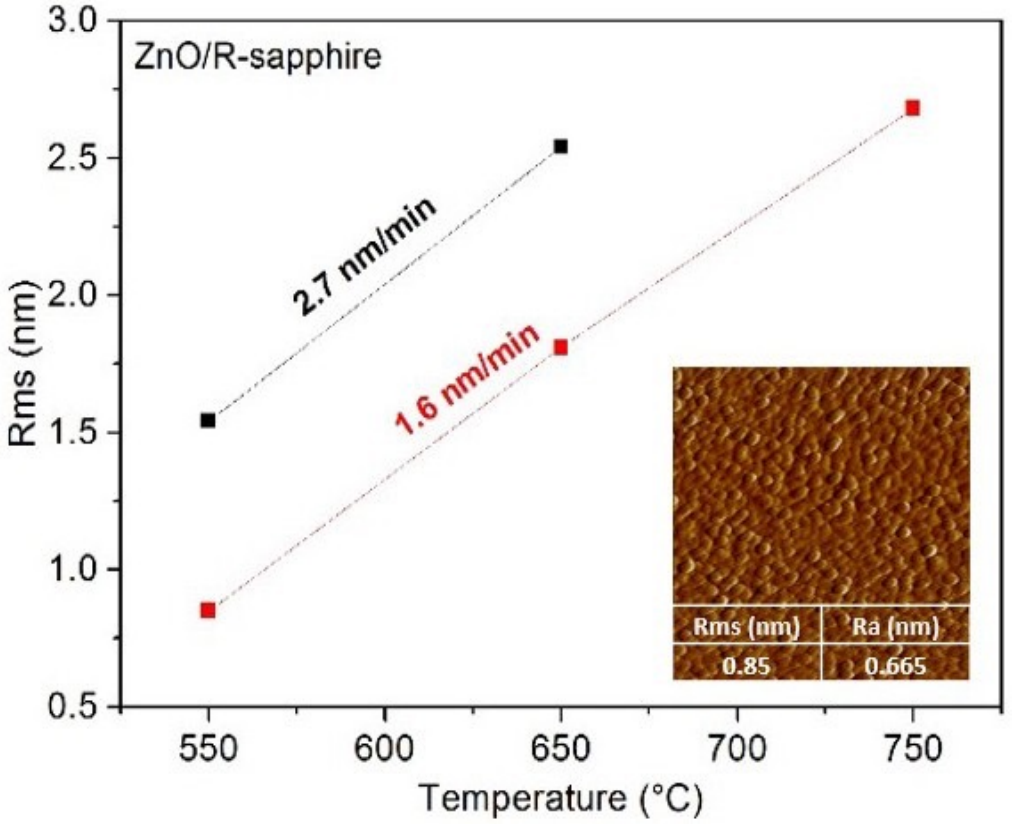

Epitaxial growth

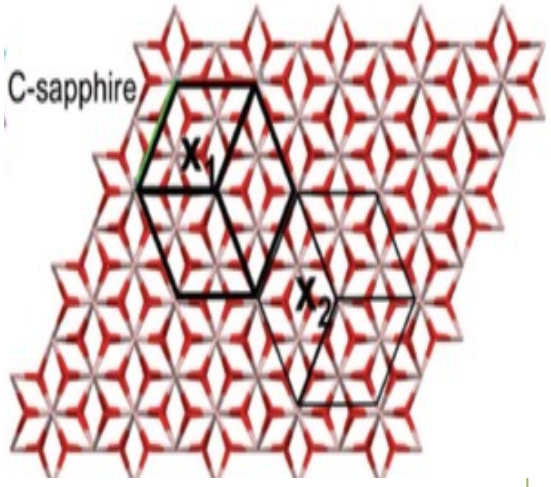

- Single crystal substrate: lattice/symmetry matching
- Slow nucleation & high surface mobility
- High temperature & slow growth rate

Surface mobility

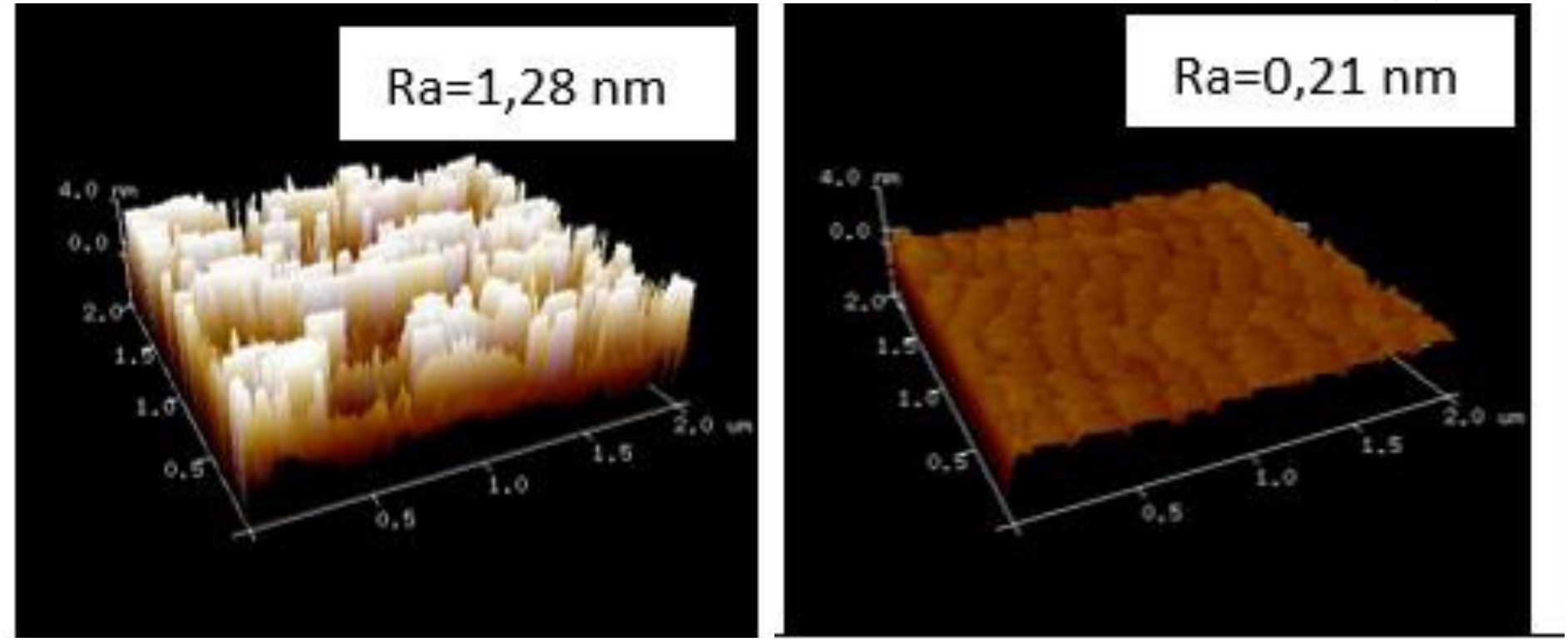

Limited number of nucleation sites (smooth surface with terraces)
Thermal energy is sufficient for diffusion (high temperature)
The collisions between adatoms rare (slow growth rate)

Nucleation and growth of thin films

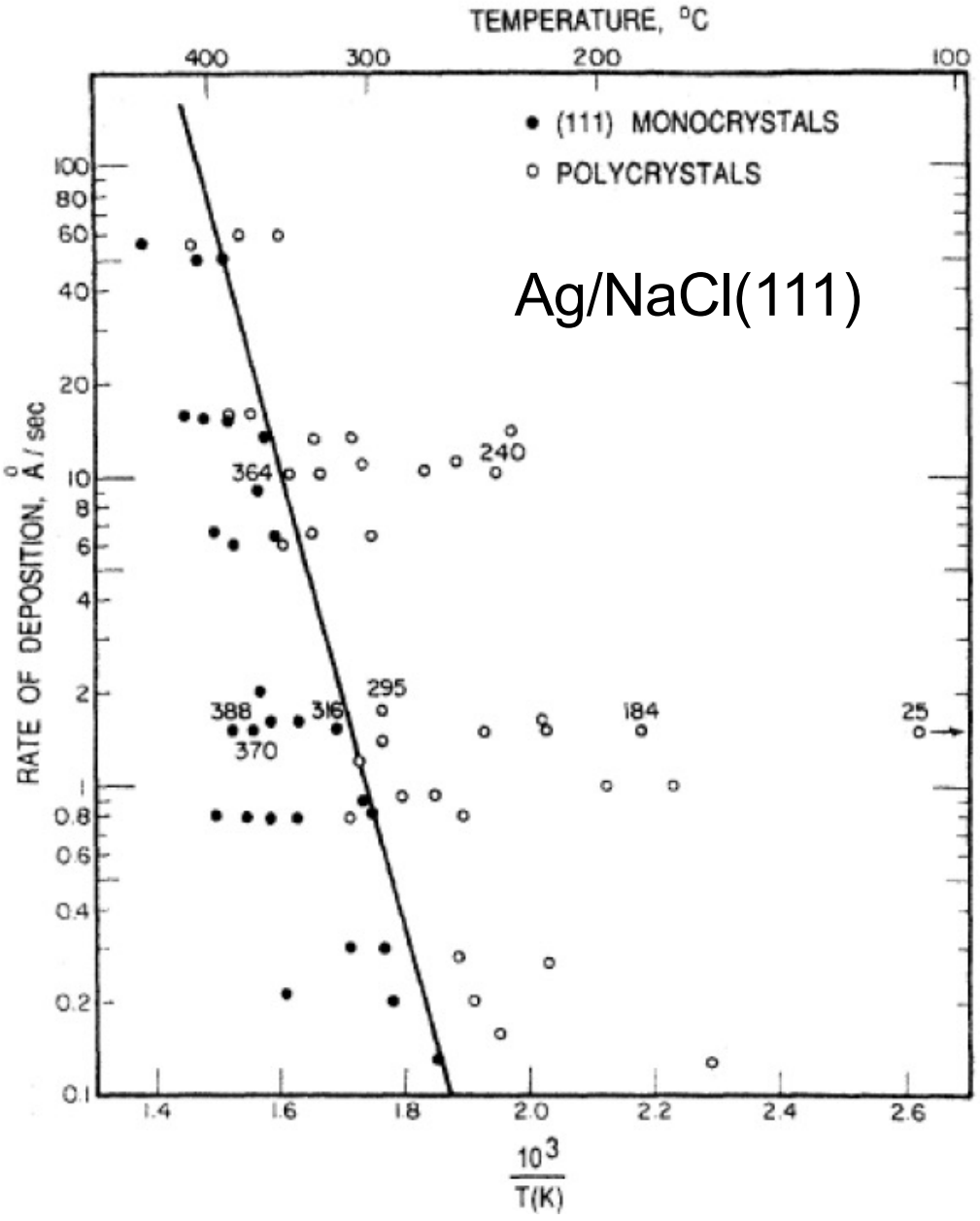

Epitaxial films

- High temperature & low deposition rate

Polycrystalline films

- Lower temperature & high deposition rate

Epitaxial or textured films

Fast growth rate, low temperature
=> Texture

Low growth rate & high energy for surface mobility
=> Epitaxy

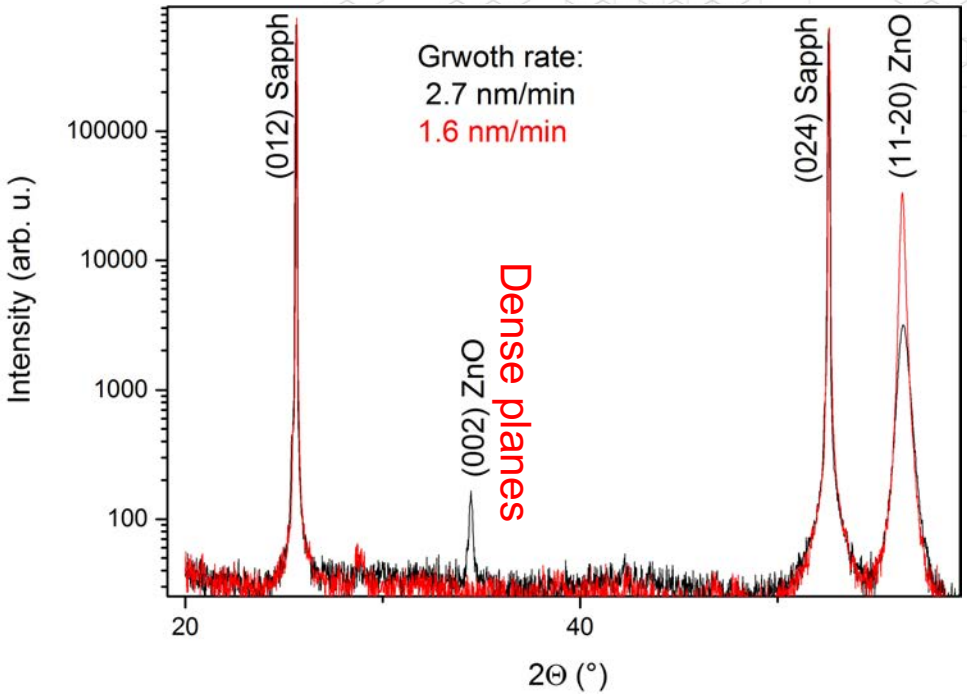

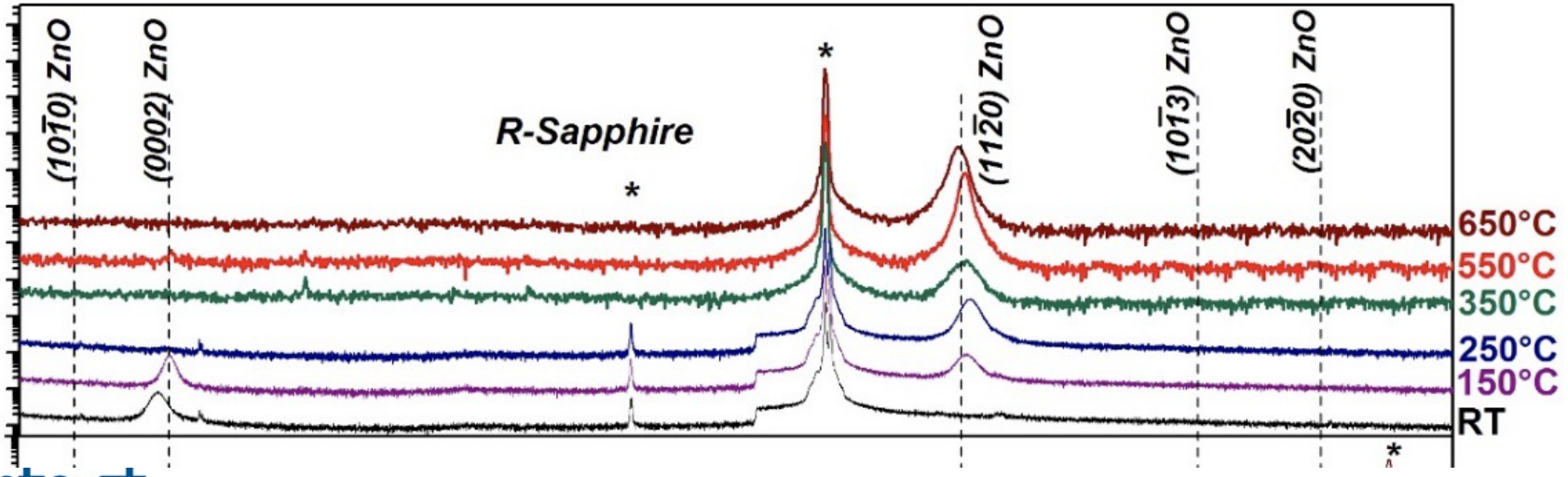

Epitaxial growth quality

Epitaxy –defined in-plane orientation / dependence on the substrate orientation

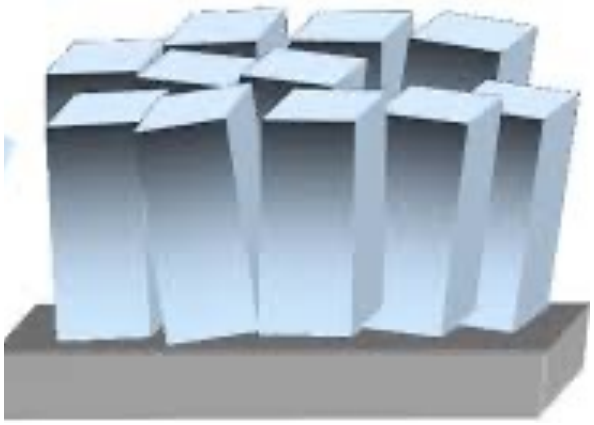

Mosaicity –dispersion of growth orientation along the normal to the substrate

Epitaxy

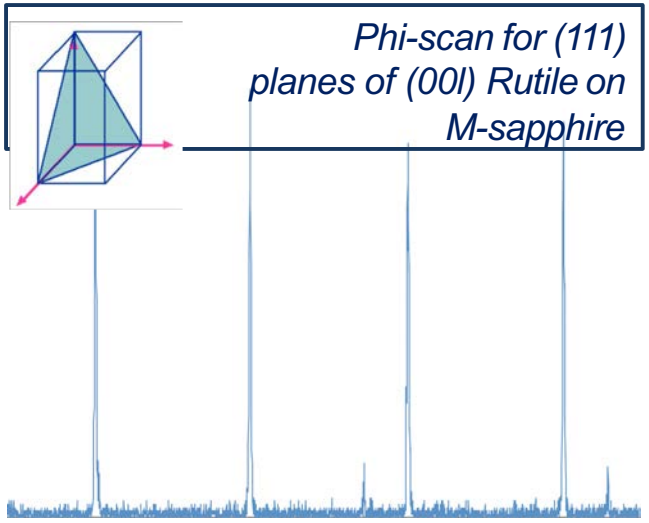

Mosaicity

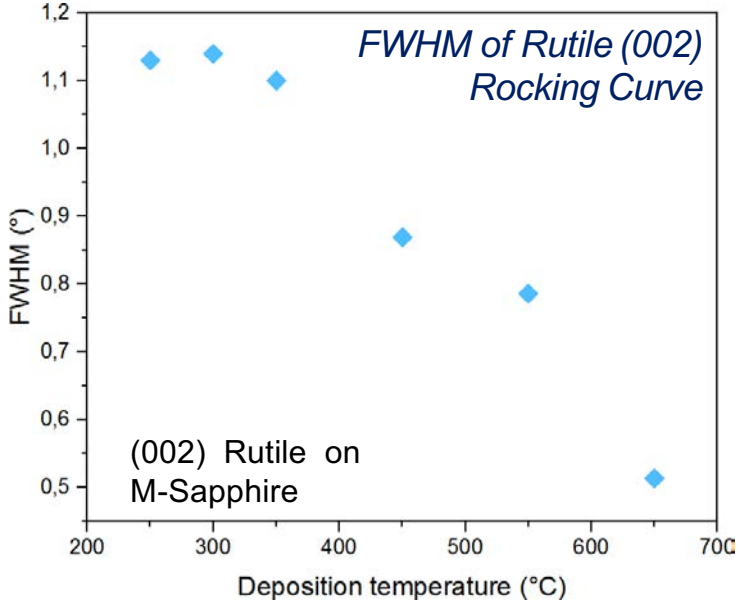

Control of the growth orientation

- Lattice mismatch
- Alignement of the dense planes
- Asymmetry of the surface planes

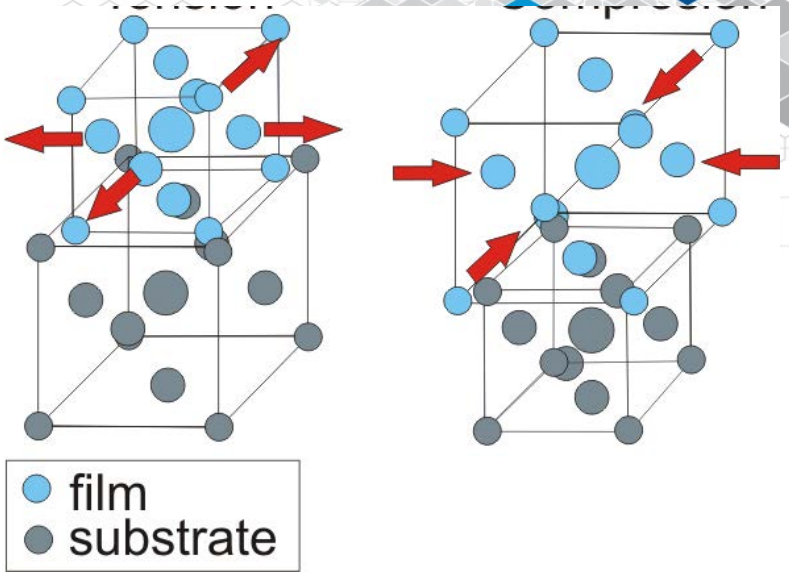

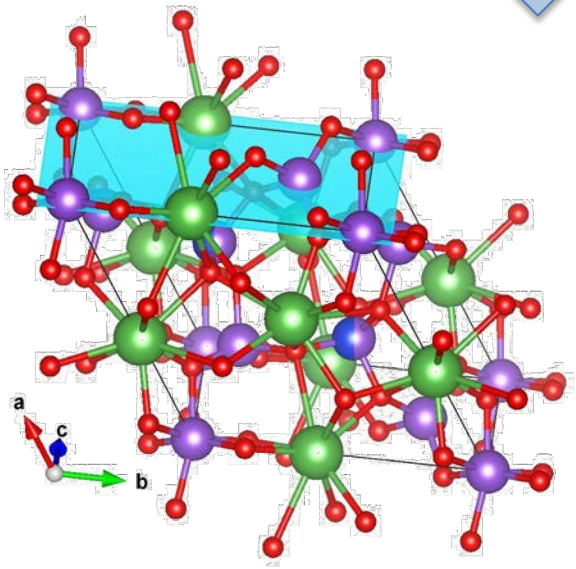

Ga^{3}

La^{3+}

$\frac{1}{2}Si^{4+}/\frac{1}{2}Ga^{3+}$

O^{2-}

Stereographic projections

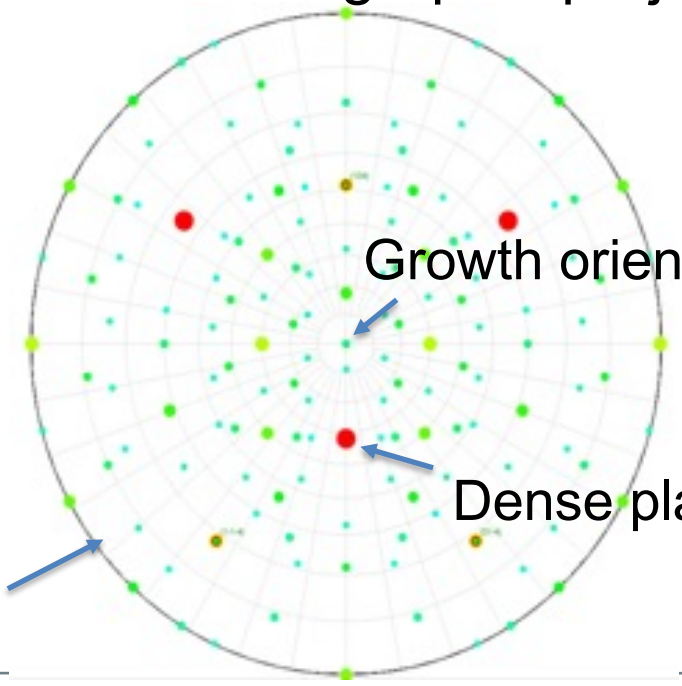

Planes perpendicular to the substrate plane

Bartasyte et al. Adv. Mater. Interfaces 2017

(10-10)-$LiNbO_3$ films

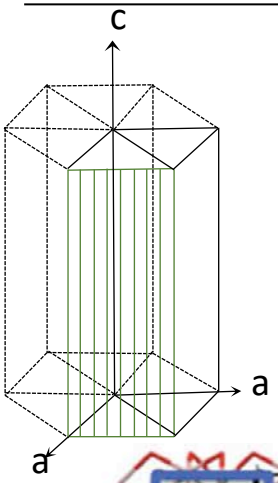

(10-10)-LN

$d_{(11\text{-}20)}$= 2.576 Å
$d_{(0006)}$= 2.310 Å

(10-10)-sapphire

$d_{(11\text{-}20)}$= 2.380 Å
$d_{(0006)}$= 2.166 Å

Best lattice mismatch:

$c_{LN}//a_{sapphire}$ $4a_{LN}//5a_{sapphire}$

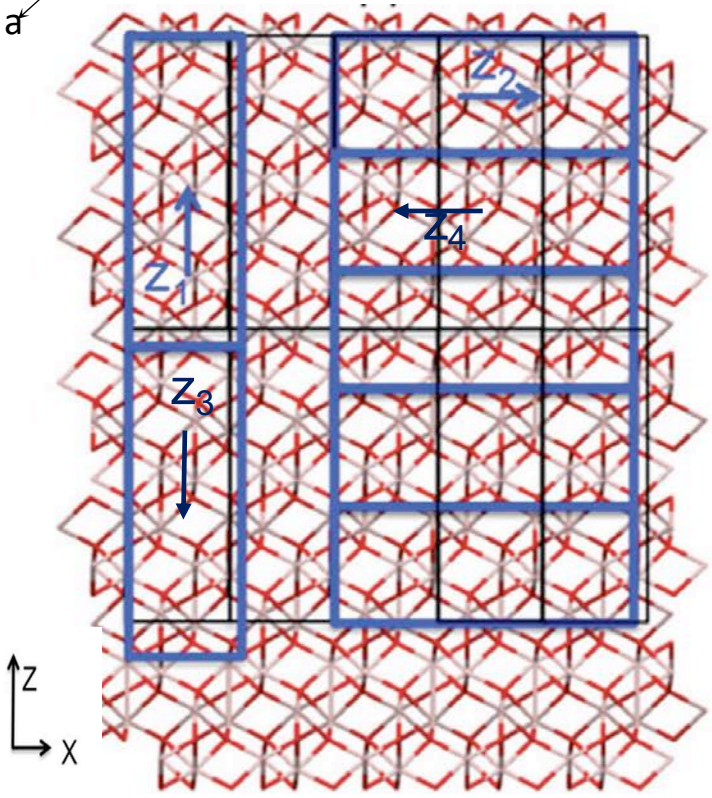

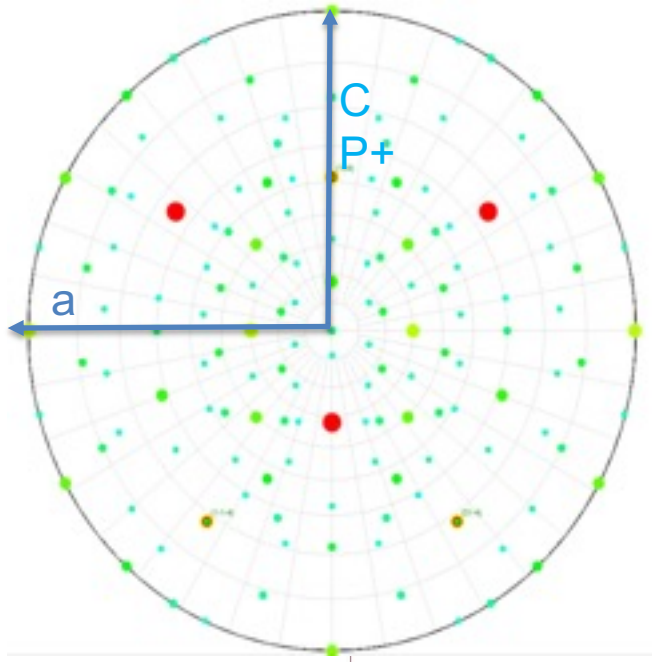

Fast growth => 4 growth domains

Slow growth => No growth domains: $a_{LN}//a_{sapphire}$ & $c_{LN}//c_{sapphire}$ (alignement of dense planes)

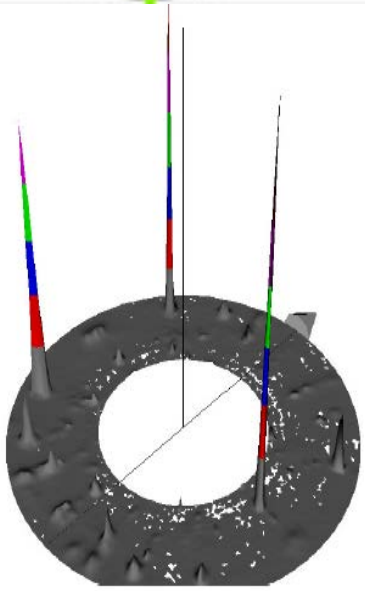

Pole figure (01-14)

(000L)-$LiNbO_3$ films

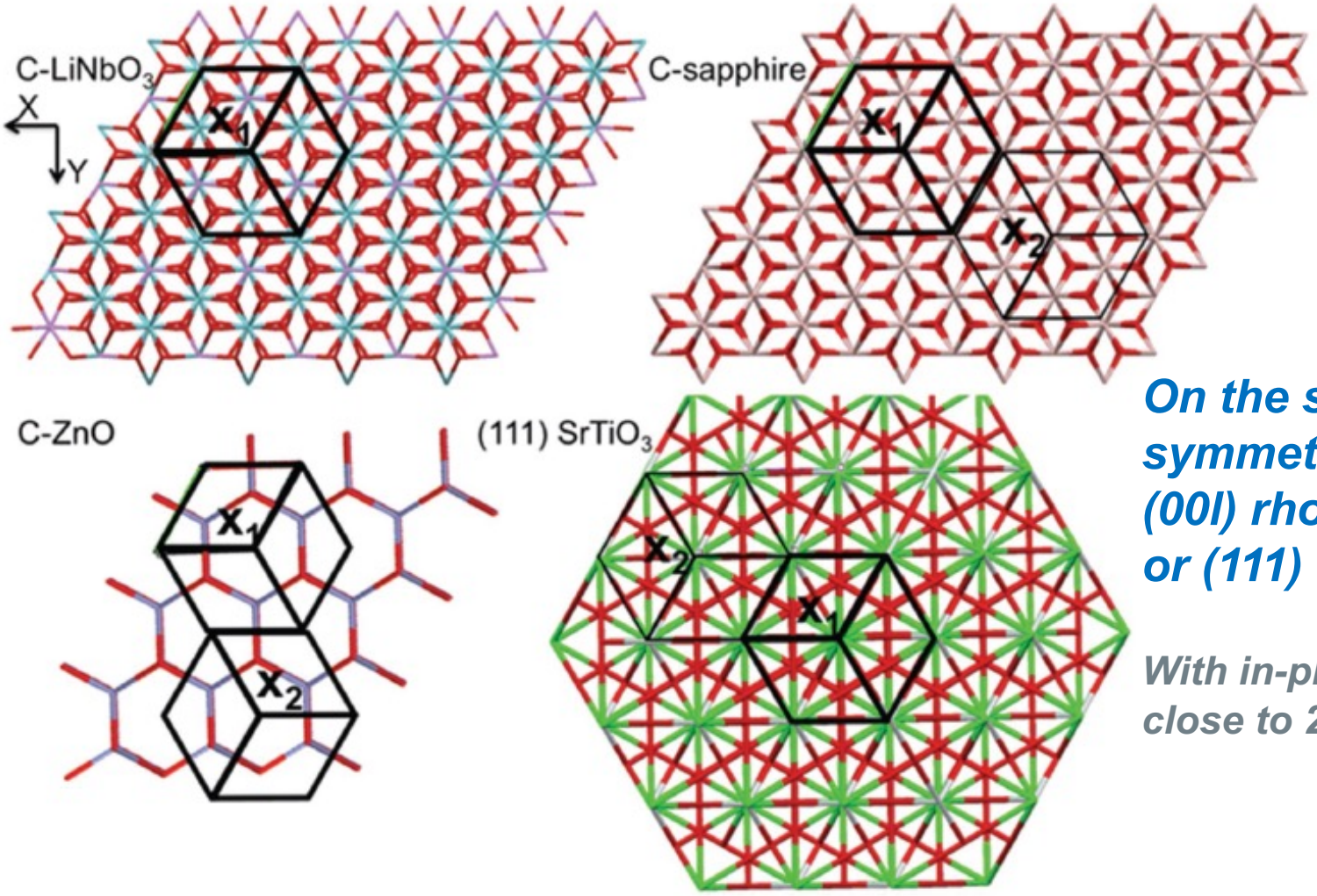

On the substrates with the symmetry « 3 » or « 6 »: (00l) rhombohedral/hexagonal or (111) cubic (Pt, $SrTiO_3$, etc.)

With in-plane lattice parameters close to 2.5 Å

A. Bartasyte et al, Review, Adv. Mater. Interfaces 2017

(000L)-$LiNbO_3$ films

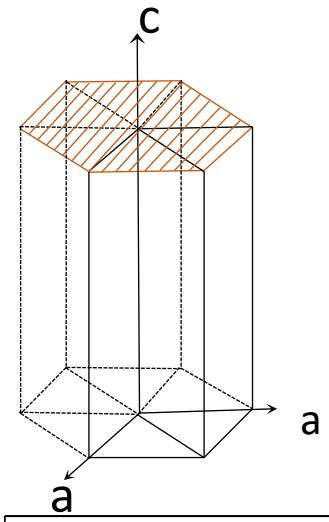

Z-LN

$d_{(11\text{-}20)}$= 2.576 Å
$d_{(30\text{-}30)}$= 1.487 Å

C-sapphire

$d_{(11\text{-}20)}$= 2.380 Å
$d_{(30\text{-}30)}$= 1.374 Å

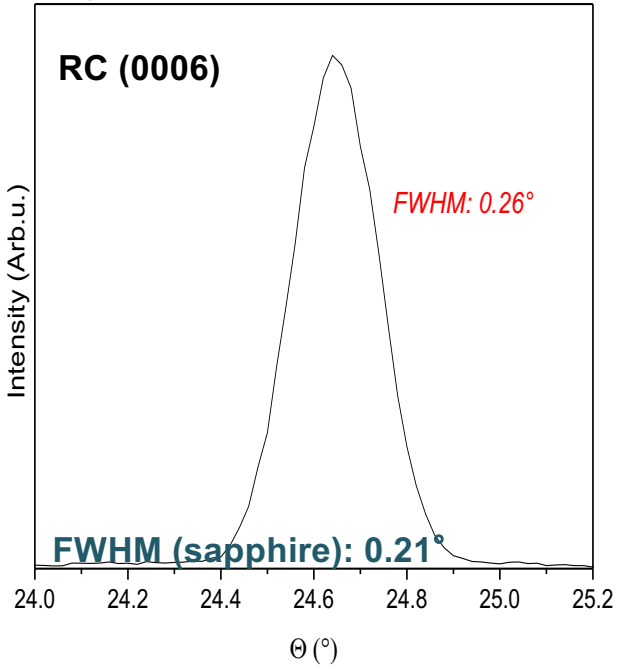

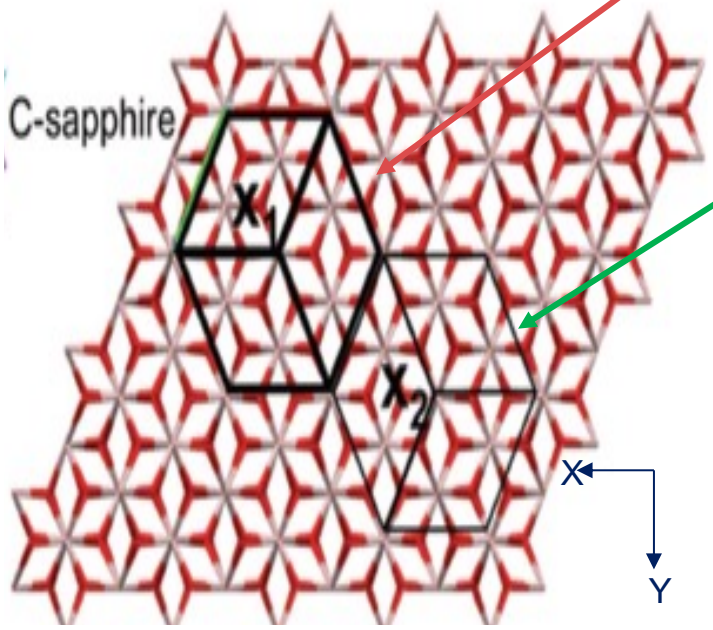

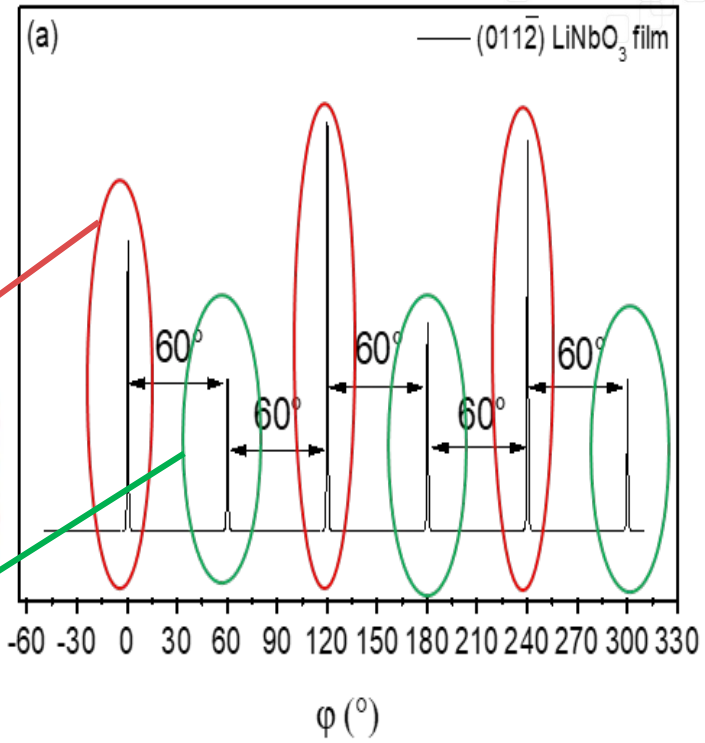

Two growth domains

Z-$LiNbO_3$ films

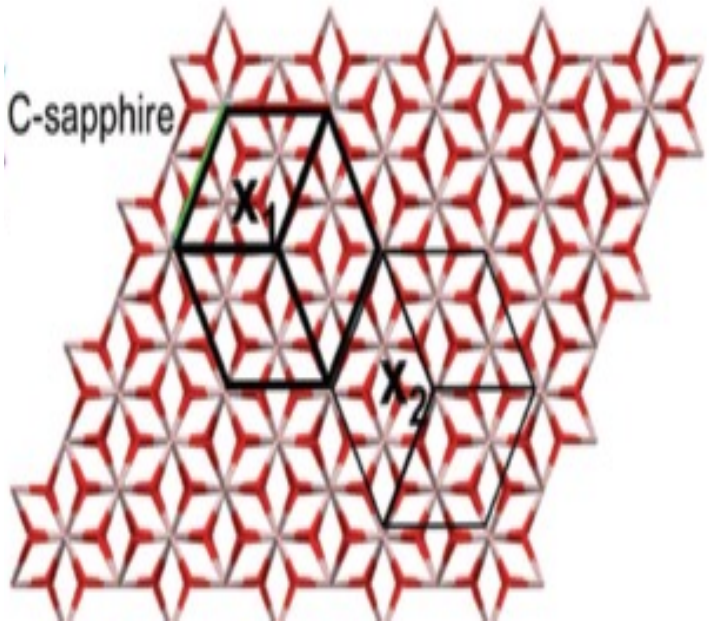

Two growth domains

⇩

Eliminated by post-annealing!

Alignment of the dense planes

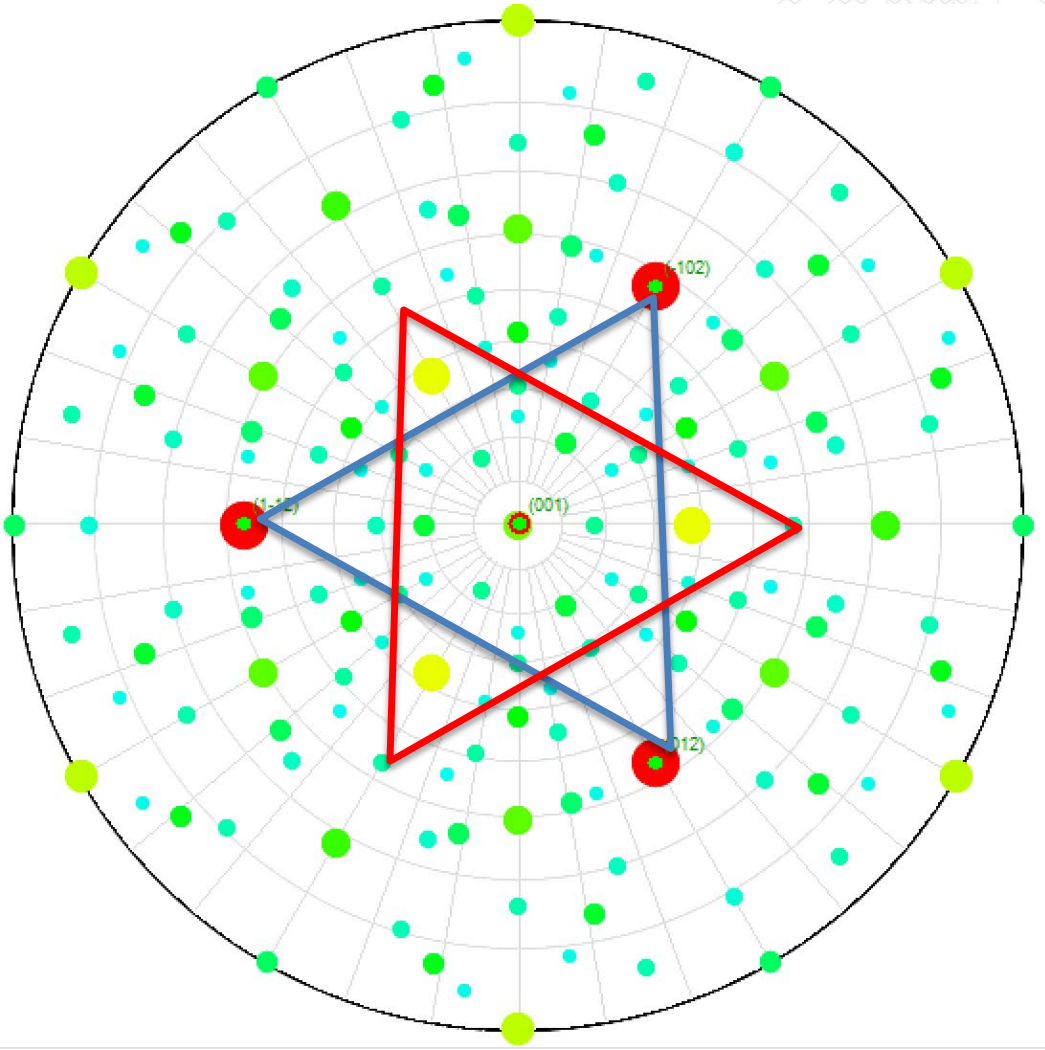

Z-$LiNbO_3$ films

C-LN on (100) YSZ (cubic substrate:

Four growth domains & defective boundaries

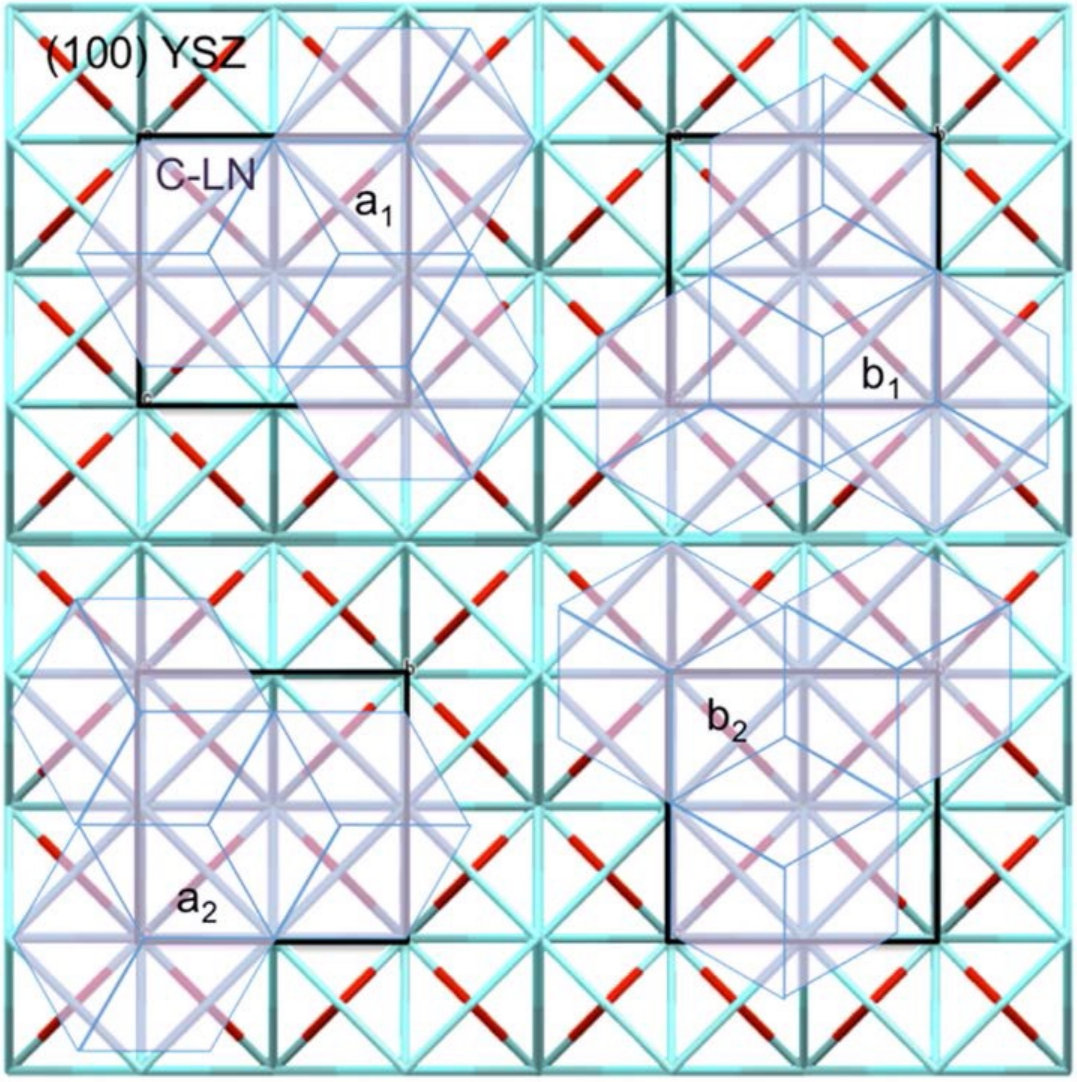

A. Bartasyte et al, Review, Adv. Mater. Interfaces 2017

(01-12)-$LiNbO_3$ films (pseudocubic orientation)

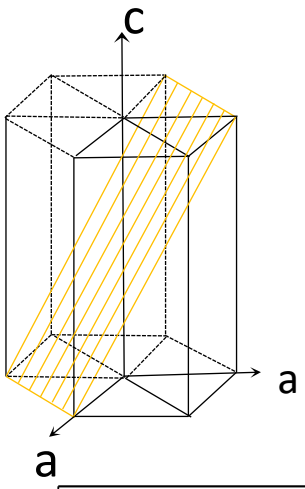

(01-12)-LN

$d_{(11\text{-}20)}$= 2.576 Å
$d_{(01\text{-}14)}$= 2.736 Å

(01_12)-$LaAlO_3$

$d_{(11\text{-}20)}$= 2.683 Å
$d_{(01\text{-}14)}$= 2.679 Å

CUBIC SUBSTRATES

- (100) $SrTiO_3$
- (100) LSAT

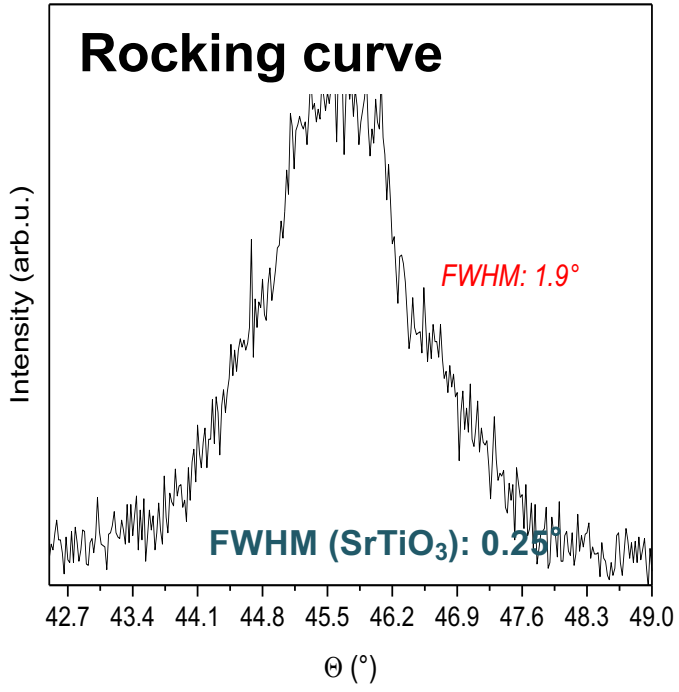

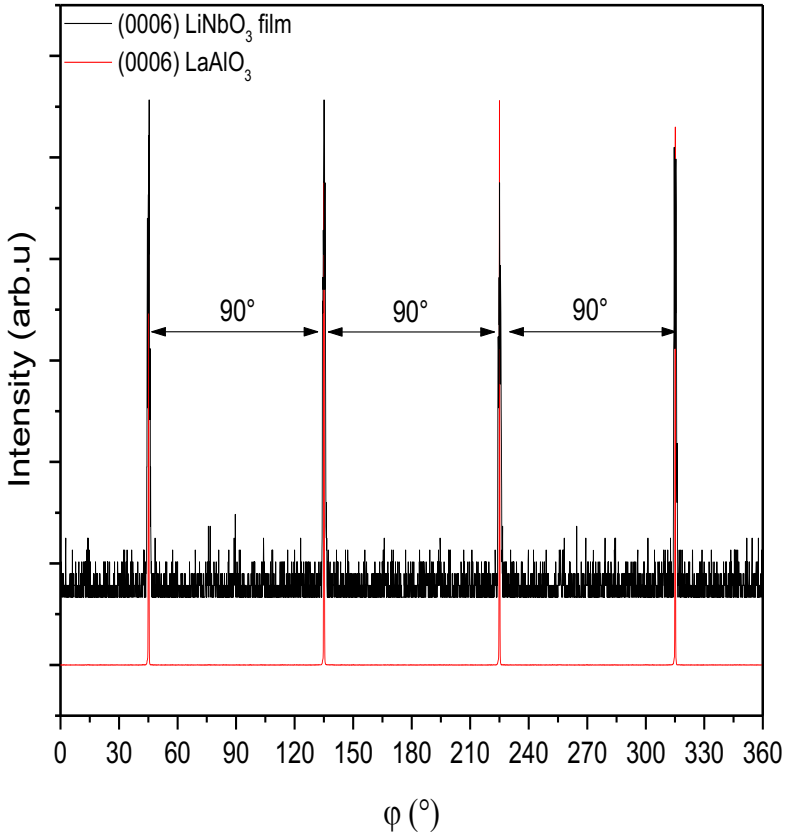

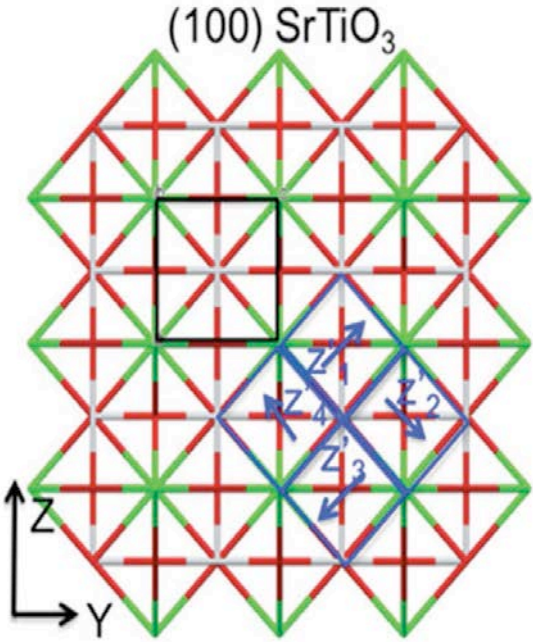

4 growth domains

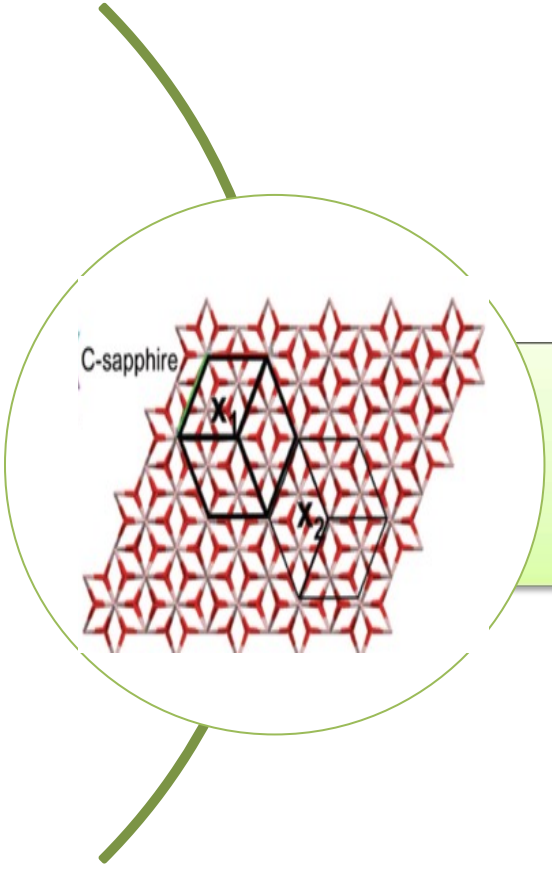

Defects & Composition

Polycrystalline vs Epitaxial

Acoustical/optical propagation losses, increased resistivity due to polycrystallinity/ grain boundaries/ surface roughness

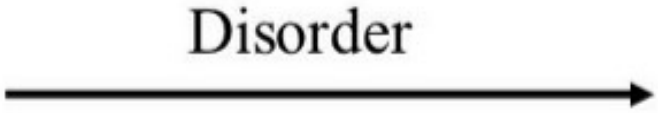

Epitaxial

Surface rougness /islands

$\neq$ *grain size*

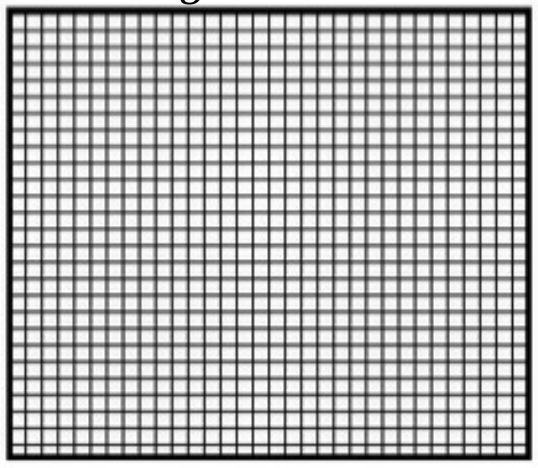

Low propagation losses

Low resistivity

Polycrystalline

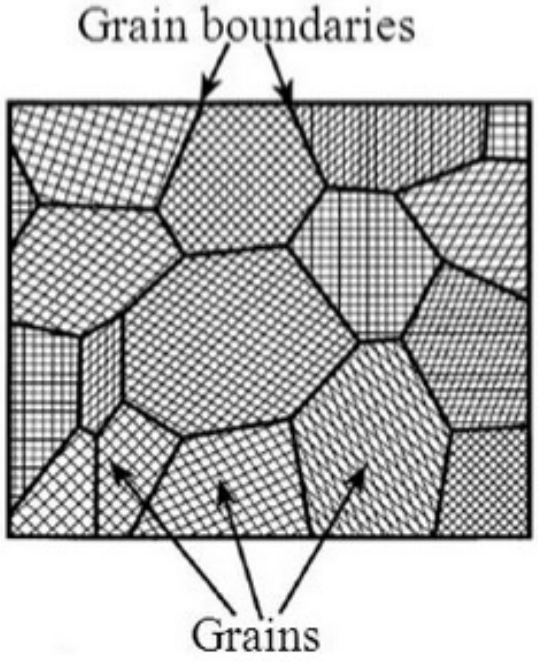

Average properties

Amorphous

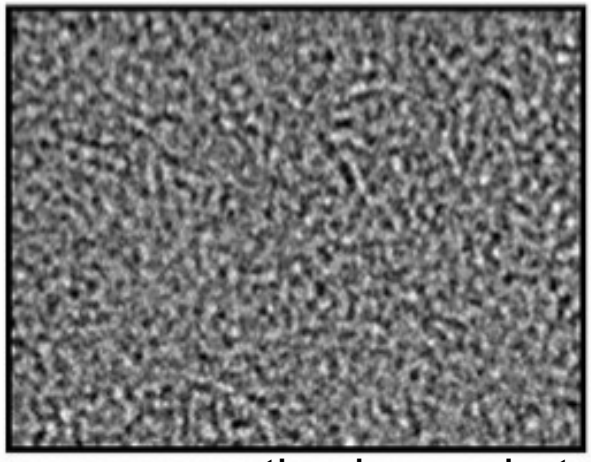

Low propagation losses but different properties (no 1st & 3rd rank properties)

B. Parsons. Solidification & Crystalline Imperfections.

femto-st SCIENCES & TECHNOLOGIES

Resistivity

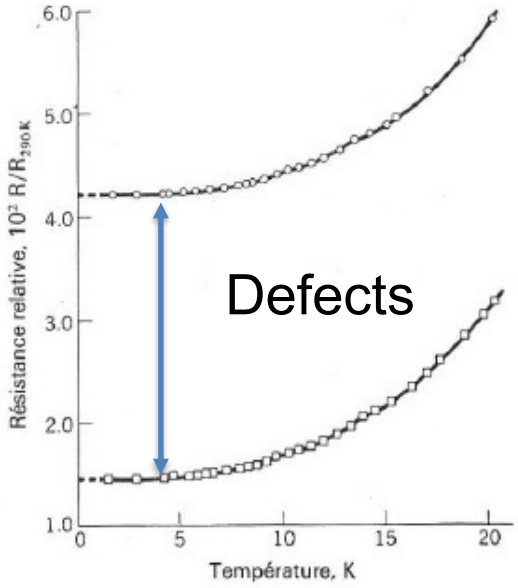

Figure 9 Résistance du potassium, au-dessous de 20 K, mesurée sur deux échantillons par D. K. C. MacDONALD et K. MENDELSSOHN, *Proc. Roy. Soc.* (Londres) **A 202,** 103 (1950). Les différentes ordonnées à l'origine ($T = 0$ K) sont attribuées aux différentes concentrations en impuretés et en défauts statiques des deux échantillons. Pour les mesures réalisées au-dessous de 4,2 K, voir D. GRIGAN, *Proc. Roy. Soc.* (Londres) **A 325,** 223 (1971).

Thin film resistivity dependent

- Composition/nonstoichiometry
- Texture/epitaxial quality
- Grain size
- Thickness

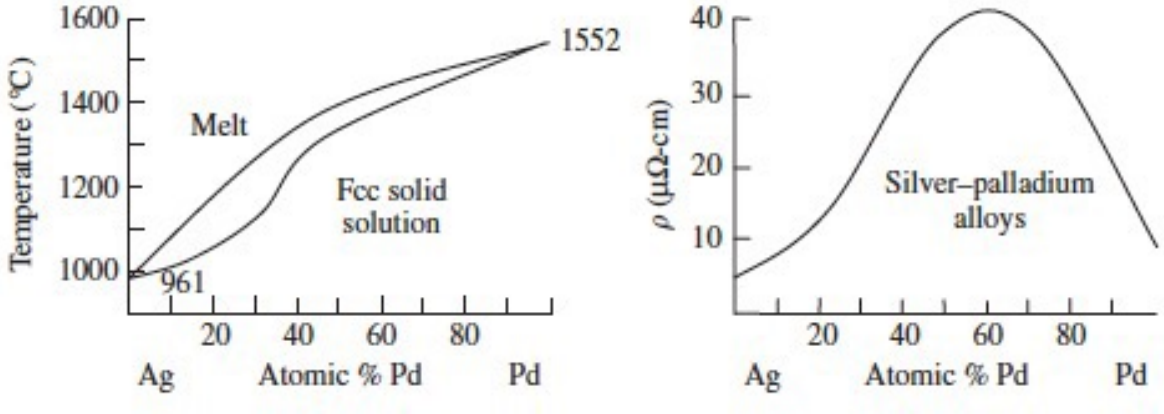

Fig. 17.3 The phase diagram and room temperature resistivity of Ag–Pd alloys used as electrodes in electroceramics. Melting points increase smoothly from Ag to Pd but the resistivity is greatest at intermediate compositions. Similar behavior is observed with many other electrode alloys including the Pd–Cu, Pd–Au, Pd–Ni, Pd–Pt, Ag–Au, and Ag–Pt systems.

Epitaxial growth defects

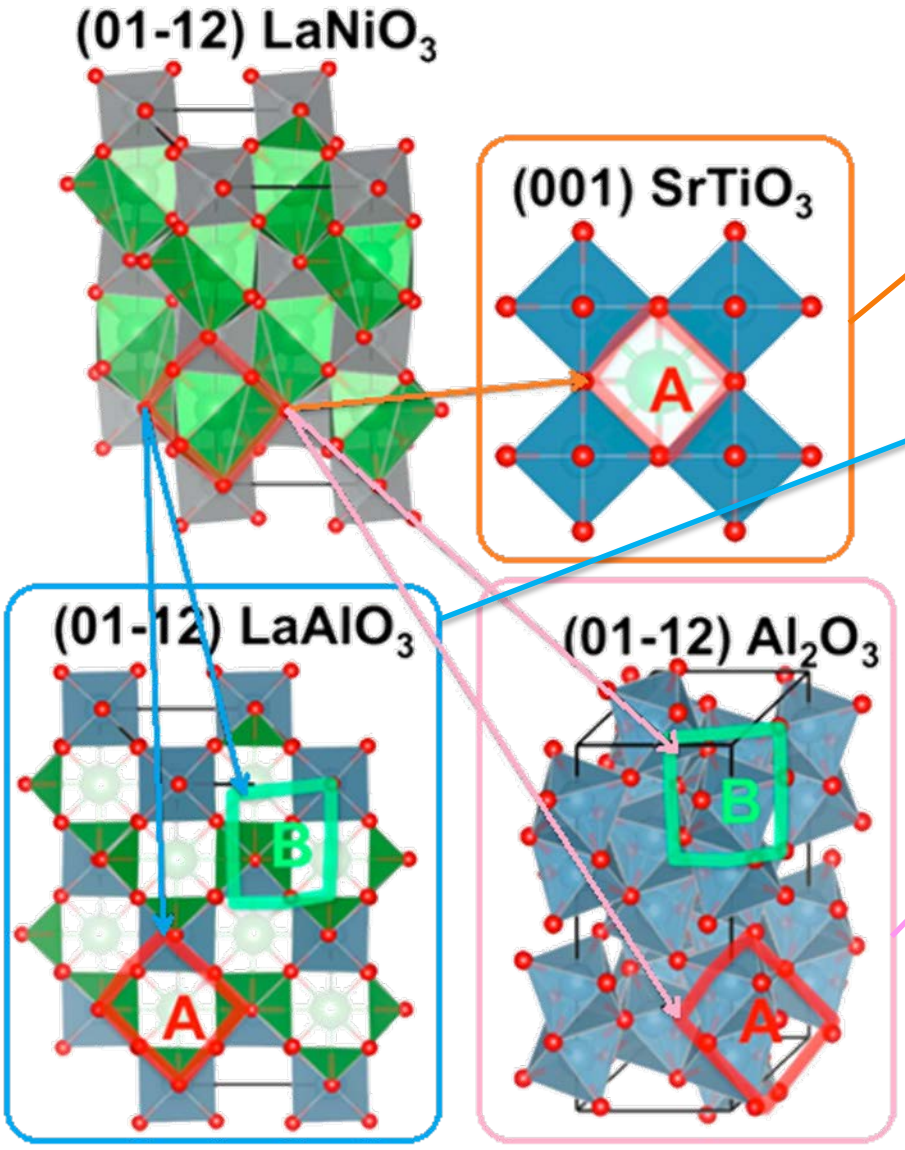

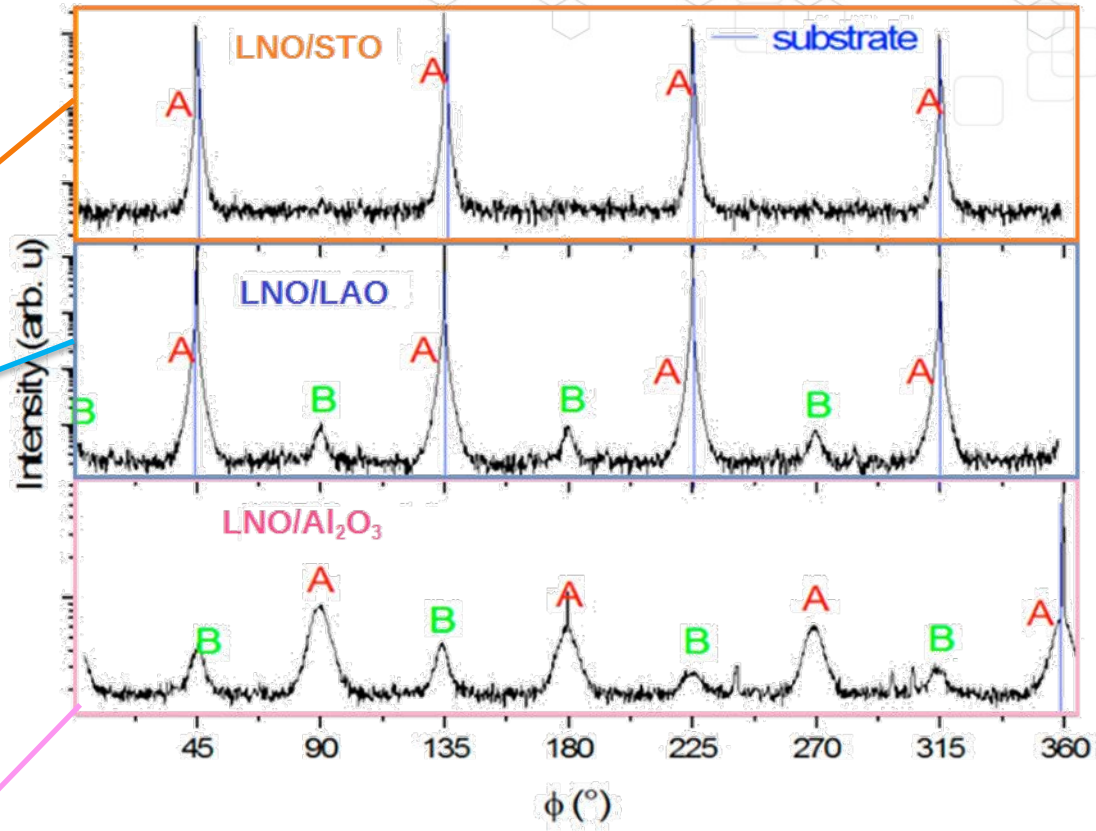

Projections of polyhedral structure of $SrTiO_3$, $LaNiO_3$, $LaAlO_3$ and Al_2O_3. The growth domains, rotated in the substrate plane by 45 ° with respect to each other, were named A and B. (**right**) XRD φ-scans of (0006)/ ($20\bar{2}2$) planes of $LaNiO_3$ films on $SrTiO_3$, $LaAlO_3$ and Al_2O_3 substrates.

Resistivity

Key parameter : Stoichiometry in oxygen, structural defects and La_2O_3-NiO ratio

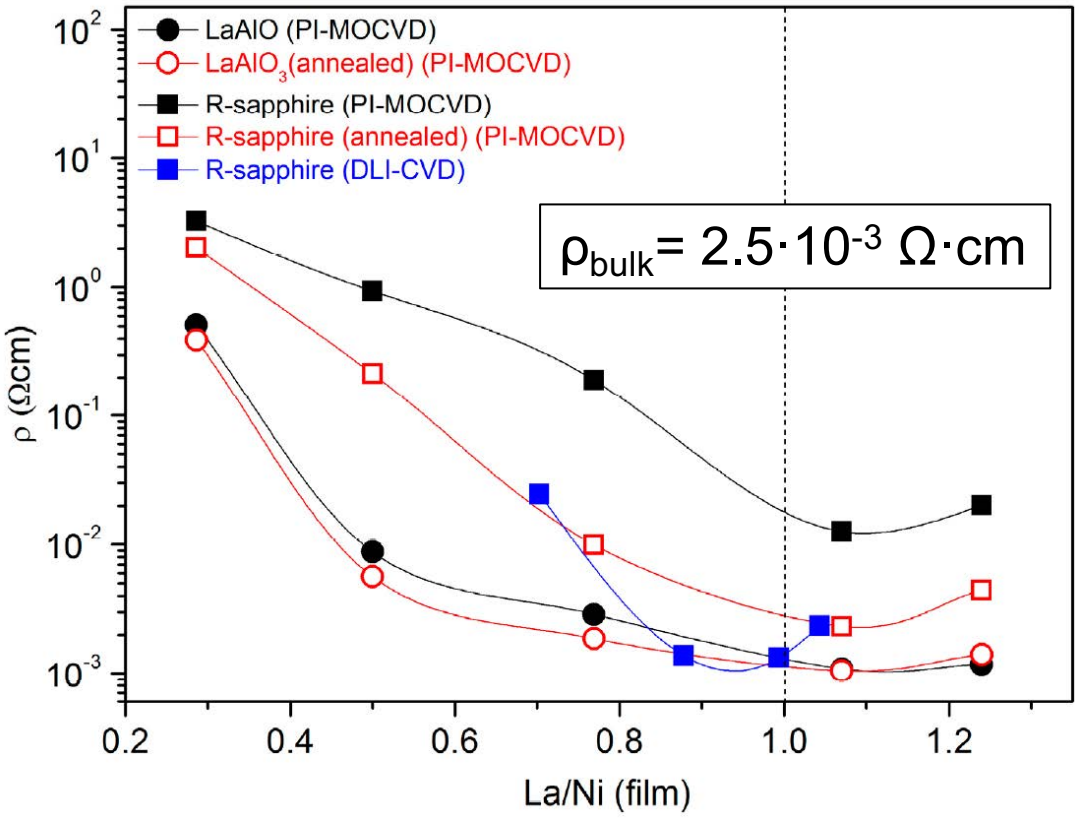

Composition dependence of resistivity of as-deposited and annealed $LaNiO_3$ films on $LaAlO_3$ and R-sapphire substrates.

- **Annealing at 750˚C in air** significantly reduced resistivity in LNO/Al_2O_3 structures (down to $2.3 \cdot 10^{-3}$ Ω·cm)
  - ➢ Recrystallization
- $1.26 \cdot 10^{-3}$ Ω·cm by direct growth on Al_2O_3 **at 750˚C !**
- La_2O_3-NiO-O stoichiometry also impacts resistivity

$\rho_{(LNO/Al2O3)} = 1.26 \cdot 10^{-3}$ Ω·cm
$\rho_{(LNO/LAO)} = 1.05 \cdot 10^{-3}$ Ω·cm

femto-st SCIENCES & TECHNOLOGIES

Kuprenaite et al. Coatings 2019

Control of volatile oxide composition

1. Increase deposition pressure

Deposition pressure (Torr)	Li2O in film (mol%)
5	48.3
10	48.6
20	49.0

2. Decrease deposition temperature

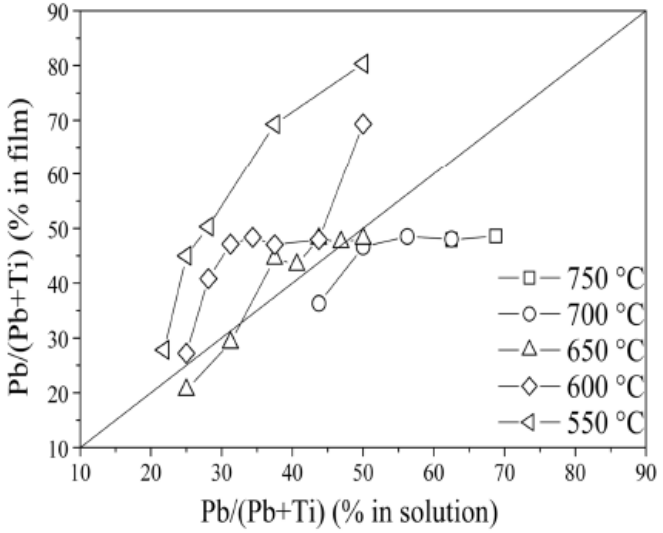

3. Increase oxygen partial pressure

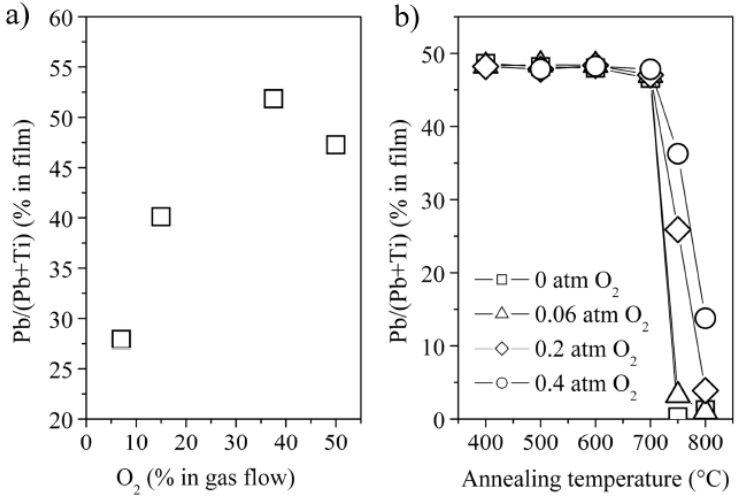

4. Increase growth rate

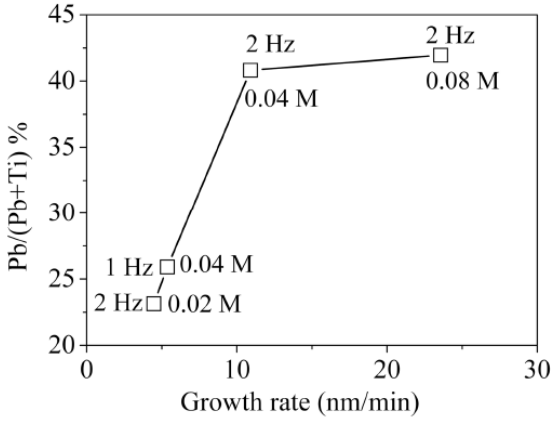

5. Compensate by target/ precursor composition

(6. Saturate atmosphere)

More details in Bartasyte et al., Review, Adv. Mater. Interfaces 2017 & bartasyte, thesis INP Grenoble 2007

Summary

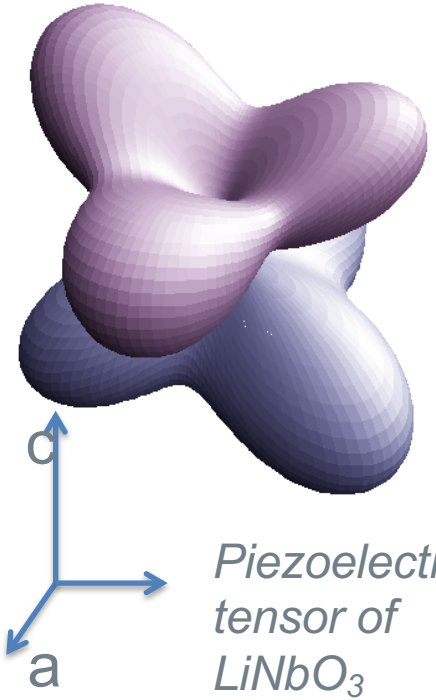

Piezoelectric tensor of $LiNbO_3$

Thank you for your attention!

femto-st SCIENCES & TECHNOLOGIES
PROJET FINANCÉ PAR L'ANR - PROJECT FUNDED BY THE ANR
EIPHI-BFC GRADUATE SCHOOL CROSS DISCIPLINARY SCIENCE AND TECHNOLOGY
Horizon 2020 Programme